Chapter 12
Biomedical Engineering Fundamentals

Ram Bilas Pachori and Vipin Gupta

If it weren't for electricity, we'd all be watching television by candlelight.

George Gobel

Contents

R. B. Pachori · V. Gupta (✉)
Discipline of Electrical Engineering, Indian Institute of Technology Indore, Indore, India
e-mail: vipingupta@iiti.ac.in

F. Firouzi et al. (eds.), *Intelligent Internet of Things*,
https://doi.org/10.1007/978-3-030-30367-9_12

12.1 Introduction of Bioelectricity and Biomechanics

In the current scenario, the innovation in technology is increasing as per the requirements of our lives. This fact is also true for the area of health-care services and medicine. The recent advancement in health-care system leads to effective diagnosis and better treatment of diseases with the help of biomedical engineering. Biomedical engineering includes two major fields, medicine and engineering. The engineering field has assisted health-care technology by providing tools and techniques such as biosensors, signal processing, image processing, and artificial intelligence. These tools and techniques help health-care technology in the research, diagnosis, and treatment of various diseases [1]. The field of biomedical engineering also includes many new areas of research such as bioelectricity and biomechanics.

Bioelectricity is also known as electrophysiology [2]. Bioelectricity has the same principle which the electricity has in the atmosphere and solid-state materials. One of the major differences in bioelectricity and electricity is that the living systems derive their electrical energy from the difference of ionic concentration which is present across cell membranes as compared to man-made electrical systems. Therefore, the energy sources in living systems are distributed in space along the membrane, and this energy can be utilized by involving a flow of current across the membrane. In other words, the systems designed by humans have a localized energy source, for example, a battery, which conducts the currents through a conductor, whereas living systems have distributed sources of energy. The bioelectricity is quantified with the help of potentials and currents which values are functions of position. The animals and people have huge volumes with conducting solution through which ionic currents can flow. Hence, the study of bioelectricity is important for understanding the electrical phenomena in different parts of a living system [3].

On the other hand, the biomechanics is a study of human movement which is defined as the interdisciplinary that describes, analyzes, and assesses human

movements [4]. Biomechanics includes the fields of engineering mechanics, biology, and physiology. The knowledge of biomechanics helps us to understand the normal and pathologic gait, mechanics of neuromuscular control, and mechanics of growth and form. This understanding plays a significant role during the development of medical diagnostic and treatment procedures. The human athletic performance has also been enhanced with the help of biomechanics [5].

There are broad varieties of physical movements involved in biomechanics such as the lifting of a load by a factory worker and the performance of a superior athlete. These cases have used the same physical and biological principles, but the specific movement tasks and level of detail change from case to case. Thus, the biomechanics is all about the highest level of assessment of human movements [4].

12.2 Biosensors

The biomedical field basically depends on the monitoring of physical parameters and chemical properties for effective outcomes. The analysis of these physical parameters is performed in centralized laboratories, which require both capital and skilled labor. However, these methods of analysis of physical parameters seem to be accurate, but they have certain disadvantages such as time consuming and inability to monitor concentrations at any instant in real-time situations. Therefore, the development of biosensors has played an important role in instant monitoring of biochemical under real-time situations which involve invasive and noninvasive methods that offer an economic, fast, and easy analytical tool. The applications of biosensors in the biomedical field have revolutionized the biomedical field with the concept of self-monitoring. Biosensor can be defined as a device which monitors the products of an enzymatic reaction in order to obtain the potentiometric response [6].

A biosensor generally has two main components: a molecular recognition or bioreceptor component and a transducer component [7, 8]. Figure 12.1 shows a typical biosensor in which an analyte is used to provide information to bioreceptor. The bioreceptor component can be an enzyme, antibody, nucleic acid, microorganism, and whole cell or tissue. The transducer component can be optical, electrochemical, and mass-based. The types of biosensors based on these two main components include temperature, light, spectrophotometry, fluorescence, and immunosensors. The description of these biosensors is given below [9].

12.2.1 Temperature Sensors

Temperature sensors are most widely used in biological systems. The temperature sensors which are especially used for the biomedical application must exhibit high sensitivity and fast response. The semiconductor-based temperature sensors fulfill

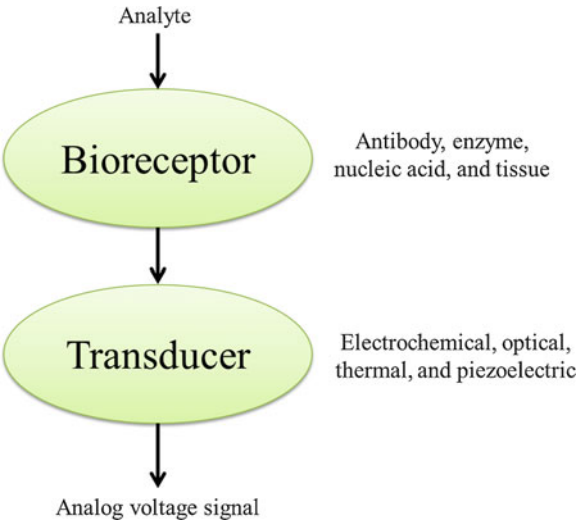

Fig. 12.1 Block diagram of a typical biosensor [9]

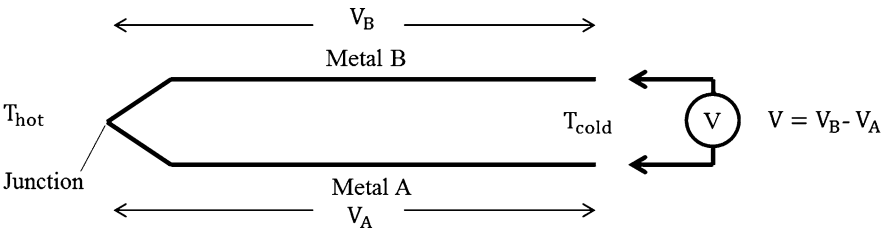

Fig. 12.2 Working principle of thermocouple [9]

the criteria of higher sensitivity compared to the others. Their response is also very fast because they are typically operated in direct contact with the medium, usually water. Hence, the semiconductor-based temperature sensors, namely, thermocouple, thermistor, diode, and transistor temperature sensors, are generally used for biomedical application and whose descriptions are as follows [9].

12.2.1.1 Thermocouple

A thermocouple consists of two dissimilar metals joined together as depicted in Fig. 12.2 [9]. The T_{hot} represents the hot junction temperature where two metals joined together while the temperature at the open junction is the cold junction temperature which is represented by T_{cold}. The temperature difference between T_{hot} and T_{cold} causes flow of heat and this heat flow creates a flow of electric current which is known as the Seebeck effect [9]. The metals used for thermocouple have some degree of resistance which will generate voltage drop V_A and V_B across metals. The difference of these voltages provides the output voltage V [9].

12.2.1.2 Thermistor

The conventional resistors may also be used as temperature sensors because the voltage drop across a resistance is inversely proportional to the temperature. A special type of resistance which is very sensitive to temperature is known as thermistor. The relationship between temperature and resistance for thermistor can be approximated through the use of the following curve-fitting equation as follows [9]:

$$\frac{1}{T} = A + B\ln(R) + C[\ln(R)]^3 \tag{12.1}$$

where T = degrees Kelvin (K), R = resistance of thermistor (Ω), and A, B, and C are curve-fitting constants. The abovementioned expression in (12.1) is called the Steinhart–Hart equation.

12.2.1.3 Diode Temperature Sensor

In the category of diodes, the Zener diode is specifically used for temperature sensing. Figure 12.3 represents the current–voltage (I-V) curve of a typical Zener diode [9]. The Zener diode is a unique type of diode which has a reverse bias configuration. The reverse bias operation of a Zener diode using negative quadrants is shown in Fig. 12.4 for understanding the working principle of Zener diode as a temperature sensor [9]. It can be observed from Fig. 12.4 that the Zener voltage is constant for a certain range of Zener currents (0.5–5 mA). This Zener voltage changes with the environmental temperature and it is linearly proportional to the temperature. On the basis of this phenomenon, we can use a Zener diode to sense temperature within a certain range of current. It is also clear from Fig. 12.4 that the high Zener current produces self-heating effect [9]. The typical working temperature range of Zener diode sensors is −400 °C to +1200 °C, which are approximately

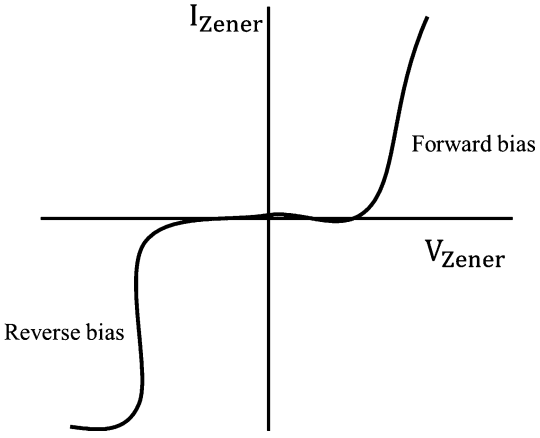

Fig. 12.3 I-V characteristic of a Zener diode [9]

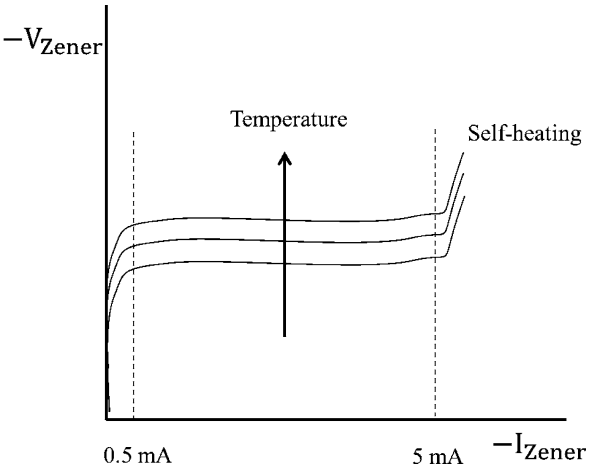

Fig. 12.4 Reverse bias V-I characteristic of a Zener diode [9]

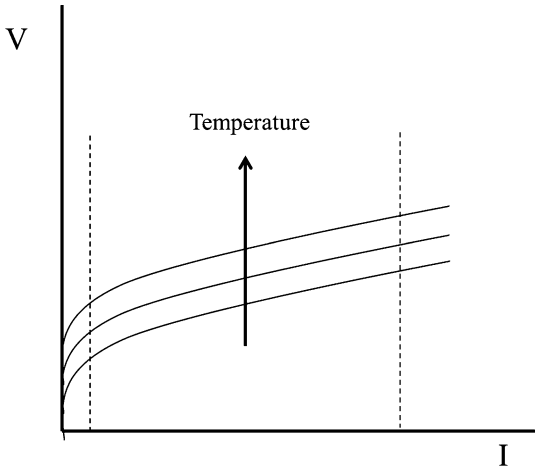

Fig. 12.5 V-I characteristics of bipolar transistor [9]

similar to the range of a thermistor. The sensitivity of Zener diode is also similar to that of a thermistor. The only benefit of a Zener diode temperature sensor is its linear operation.

12.2.1.4 Transistor Temperature Sensor

The collector current and base–emitter voltage characteristic of a transistor is very similar to reverse bias V-I characteristic of Zener diode and it can be seen in Fig. 12.5. The base–emitter part (P-N) of a bipolar transistor is actually a diode (P-N), and if we join the base and collector terminals, the bipolar transistor behaves very similar to a diode. The operating temperature range is same as that of a Zener diode and it also gives linearity over a range of temperatures [9].

12.2.2 Light Sensors

Light sensors are very important in many biosensor applications and are commonly used in conjunction with fluorescent dyes. Light is basically a part of electromagnetic radiation which is visible to the eyes of humans, and it is known as visible light. The word light is also used for some other electromagnetic radiations which are not visible to the eyes of humans such as ultraviolet (UV) or infrared (IR). The existence of light is basically in tiny energy packets which are known as photons. The properties of waves and particles are exhibited by photons. In light, the waves are sinusoidal and its peak-to-peak distance is called wavelength (λ). The wavelength of light determines its color in visible light range. A light contains a single wavelength (monochromatic) or multiple wavelengths (polychromatic). The speed of light in vacuum is always constant and its value is 3×10^8 m/s [9].

The light sensors which are made out of semiconductors are photoresistor, photodiode, and phototransistor, and the descriptions of these light sensors are as follows [9].

12.2.2.1 Photoresistor

A photoresistor is a photoconductive cell which conducts only when it is exposed to light. The semiconductor materials used for making photoresistor are cadmium sulfide (CdS), lead sulfide (PbS), and cadmium selenide (CdSe). Figure 12.6 shows a conventional photoresistor which conducts with the exposure of light. The photoresistor is usually S-shaped in order to increase the area of light exposure. In the photoresistor, the holes and electrons are bound together, and when the light (i.e., photons) is exposed to these photoresistor materials, this process creates extra electrons. Therefore, these extra electrons provide extra energy which can make the material more conductive and lowers its resistance. The mechanism in photoresistor is somewhat similar to that of a thermistor [9].

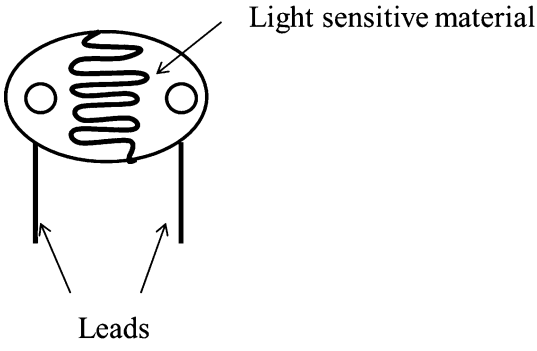

Fig. 12.6 Photoresistor [9]

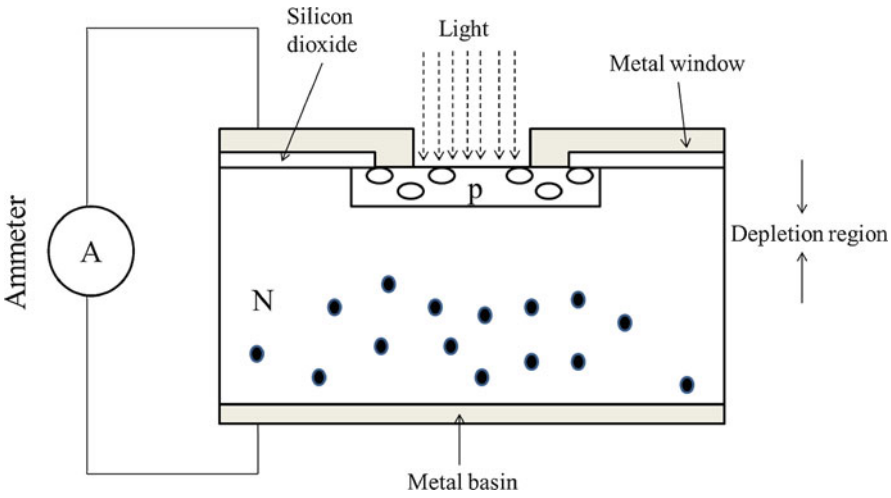

Fig. 12.7 Photodiode in photovoltaic mode [9]

12.2.2.2 Photodiode

A diode which is sensitive to photons is known as photodiode. A photodiode can be used without or with the applied voltage in order to sense light. A photodiode is constructed with a very thin P-type semiconductor which is diffused into the N-type semiconductor. The P-side of photodiode is exposed to light during operation. The mechanism of photodiode without applied voltage is shown in Fig. 12.7. This mode of operation of photodiode is also known as photovoltaic. In Fig. 12.7, the N-type semiconductor contains free electrons and P-type semiconductor contains holes. The electrons and holes repel each other. Thus, a small depletion region is formed between them. This depletion region resulted in a "less conductive" region. The sufficient supply of photons filled the depletion region with extra holes and electrons. Therefore, the depletion region will start conducting and a noticeable electric current will flow between these two semiconductors which can be observed with an ammeter [9].

12.2.2.3 Phototransistor

A phototransistor is basically a transistor which produces high current as compared to photodiode when exposed to light. The phototransistor can be constructed in two different manners which are NPN and PNP phototransistors. In an NPN phototransistor, the base current is replaced with light which provides significant energy to jump the electrons and holes from emitter to collector and vice versa. Figure 12.8 shows an NPN phototransistor which is fabricated by diffusing P-type semiconductor (base) into the N-type semiconductor (collector), followed by

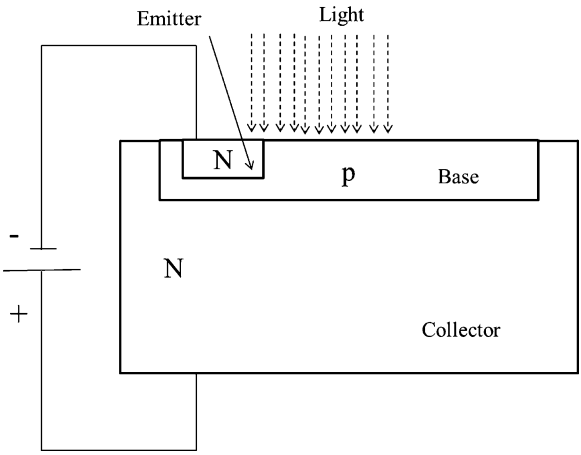

Fig. 12.8 An NPN phototransistor [9]

diffusing the N-type (emitter) into the P-type. A phototransistor has also a built-in amplifying ability [9].

12.2.3 Spectrophotometry

A spectrophotometer measures the light intensity which is transmitted or absorbed through a material. This material may be a liquid solution or gas in a container. This measure can be performed for a specific color (wavelength) or a range of colors (wavelengths). If the measurement is observed for a specific color, then it is known as photometry. On the other hand, if the measurement is observed for a range of colors, then it is known as spectrometry. This measure provides us a light intensity–wavelength curve which is called a spectrum (or spectra) [9].

The principle of absorption is most commonly used in spectrophotometer because it has certain applications in biomedical field. Figure 12.9 shows a schematic of a simple spectrophotometer. In Fig. 12.9, the source of light is a lamp which generates light of all colors in approximately equal proportions resulting in a white light source. This white light is transmitted through a monochromator which consists of a prism and a slit. The slit passes a particular color of light and this selected beam of light finally passes through a rectangular container that holds a liquid solution or gas mixture. The liquid solution or gas mixture attenuates the light intensity and the attenuated light intensity hits on the surface of photodiode which provides a current corresponding to attenuated light intensity. The absorbance A can be calculated by comparing this light intensity (l) with that from the light source (l^0) [9]:

$$A = \log\left(\frac{l^0}{l}\right) \tag{12.2}$$

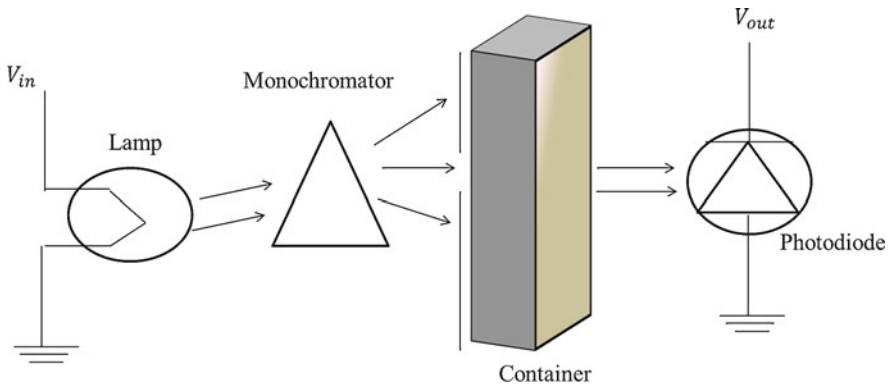

Fig. 12.9 A simple spectrophotometer [9]

where l = attenuated light intensity and l^0 = light intensity from the light source.

12.2.4 Fluorescence

The fluorescence principle is based on the absorption spectrophotometry in which we change the solute in a solution with fluorescent dyes. The color of emitted light from the container is shifted to longer wavelength. The term fluorescence was derived from the mineral fluorite, which is largely calcium fluoride. In fluorescence, the light irradiation excited the molecules and placed them in unstable excited states. The excited molecules lose their excessive energy due to their unstable nature, and this process requires emitting of the photons at the identical wavelength as that of initial light irradiation [9].

The commonly used example of fluorescence is a fluorescent lamp. In a fluorescent lamp, the charged tube of mercury vapor is used to produce ultraviolet (UV) light upon applying electrical voltage. The fluorescent coating is applied to the inner surface of the tube in order to absorb UV light and emit visible light [9].

12.2.5 Immunosensors

Biosensors which use antibodies or antigens as bioreceptors are called immunosensors. Immunosensors are widely developed for medical and veterinary diagnostics, food safety, and environmental monitoring because antibodies are very specific to proteins, viruses, bacteria, cells, etc. In comparison to other biosensors, the immunosensors are provided good sensitivity and specificity. Immunosensors have

become very popular recently [9], although the use of antibodies in biological assays has been a very common analysis in laboratory.

12.3 Basics of Signals and Systems

The signal definition plays a very important role in understanding the behavior of signal processing algorithm and its interpretation. The signal can be represented as a function of independent variables and these independent variables can vary from one to many. In other words, signal can be considered as a physical quantity which varies with respect to these independent variables and this physical quantity also contains some kind of information and behaves as a function of one or many independent variables.

12.3.1 Types of Signals

The major classification of signals is as follows [10].

12.3.1.1 Continuous, Discrete Time, and Digital Signals

The signals which have continuous amplitude and continuous time are known as continuous signals. These signals are also known as analog signals and such signals are defined at any point of time. These signals are generally denoted by $f(t)$ where f is a function which depends on the continuous variable t which is continuous in nature. Figure 12.10 shows an example of continuous-time signal.

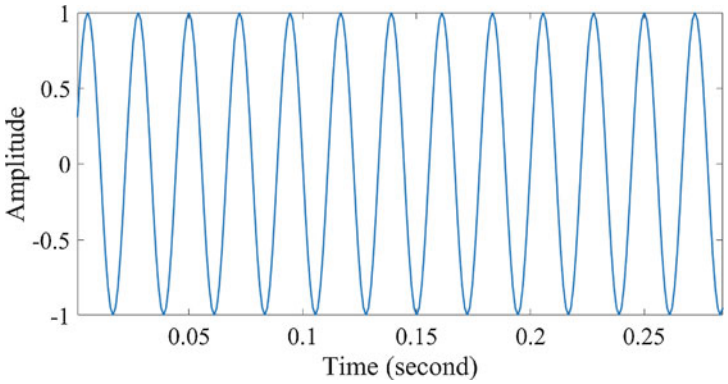

Fig. 12.10 Continuous-time sinusoidal signal

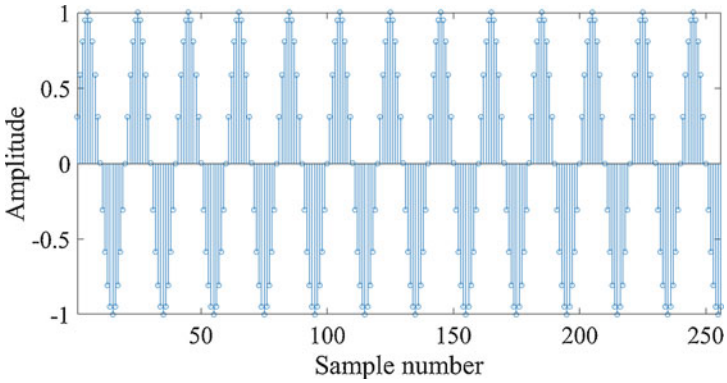

Fig. 12.11 Discrete-time sinusoidal signal

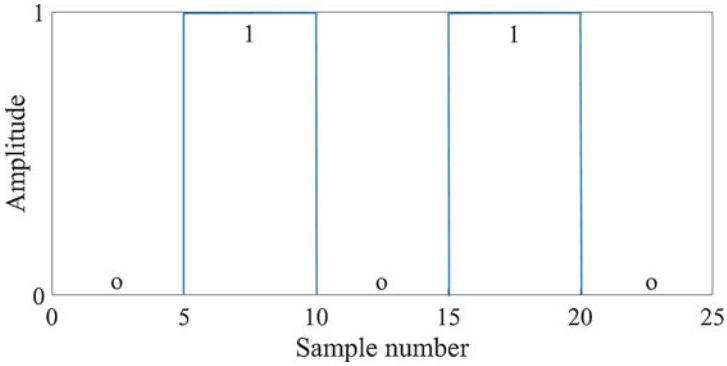

Fig. 12.12 Digital signal

Discrete-time signals have discrete time and continuous amplitude. In these signals, discretization of time is performed using sampling theorem on analog signals. Many signals are discrete signals based on the nature of their measurement. For example, if we measure the weight of a person every day for 1 month, then the plot of weight with respect to whole 30 days can be considered as a discrete-time signal. Such signals are represented by $x[n]$. The small n indicates time index or discrete time which is corresponding to the actual time $t = nT$, where T is the sampling interval. Here, n is also known as normalized time. Discrete-time signals can be also represented in the form of sequences. Figure 12.11 shows an example of discrete-time signal.

The digital signals are those signals which have discrete time and discrete amplitude. These signals have a finite number of values. For example, binary digital signal will have only two values either zero or one. The analog to digital converter (ADC) process can be used to obtain digital signal from the analog signal. Figure 12.12 shows an example of digital signal.

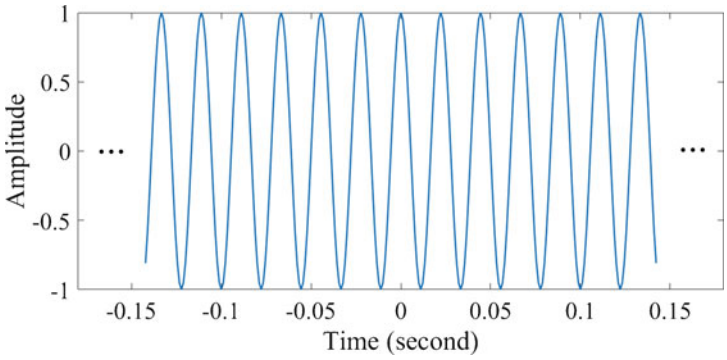

Fig. 12.13 Periodic cosine signal

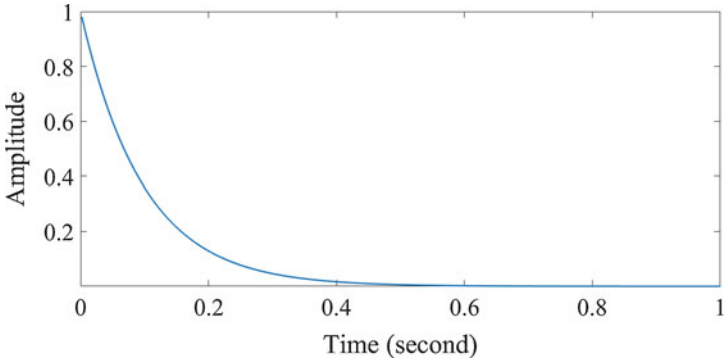

Fig. 12.14 Aperiodic exponential signal

12.3.1.2 Periodic and Aperiodic Signals

The signal which follows repetition after a time interval is known as periodic signal. For a given signal $x(t)$, it can be mathematically expressed as follows:

$$x(t) = x(t + T) \tag{12.3}$$

Here, T is known as the period of the signal.

Sine and cosine waves are examples of periodic signals and Fig. 12.13 shows an example of periodic cosine signal.

On the other hand, the aperiodic signal does not satisfy the abovementioned condition in Eq. (12.3). An example of aperiodic signal is shown in Fig. 12.14.

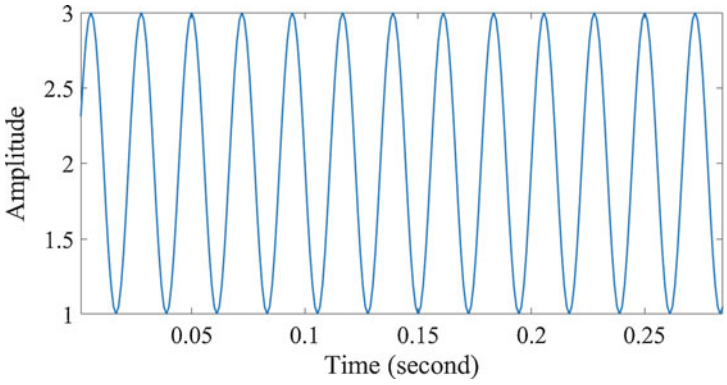

Fig. 12.15 Deterministic cosine signal

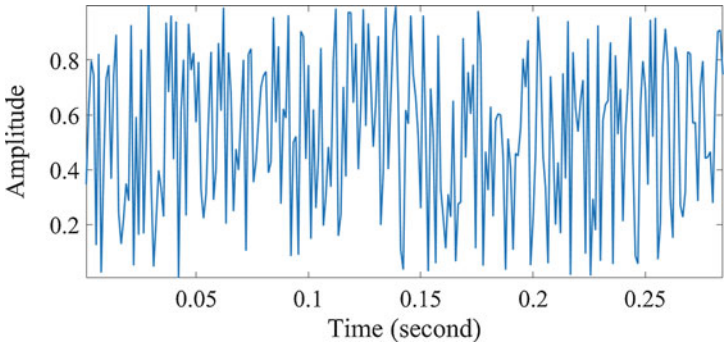

Fig. 12.16 Random noise signal

12.3.1.3 Deterministic and Random Signals

Deterministic signals are those signals which can be represented by mathematical expression and such kind of signals are well determined at any point of time. Sine, cosine, and exponential signals are examples of deterministic signals. Figure 12.15 shows an example of a deterministic signal.

On the other hand, random signals are nondeterministic signals which include uncertainty in the signal values at some point of time. For representation of such kind of signals instead of mathematical representation, they require probabilistic models. Random noise is an example of random signal. Figure 12.16 shows a random noise generated in Matlab.

12.3.1.4 Even and Odd Signals

Even signals $x(t)$ satisfy the following condition:

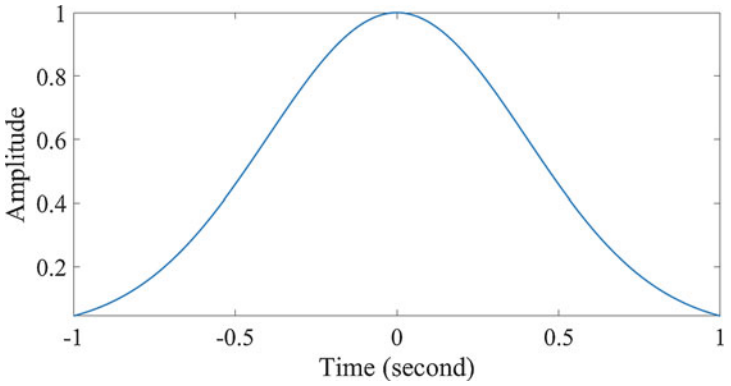

Fig. 12.17 Even signal (Gaussian window)

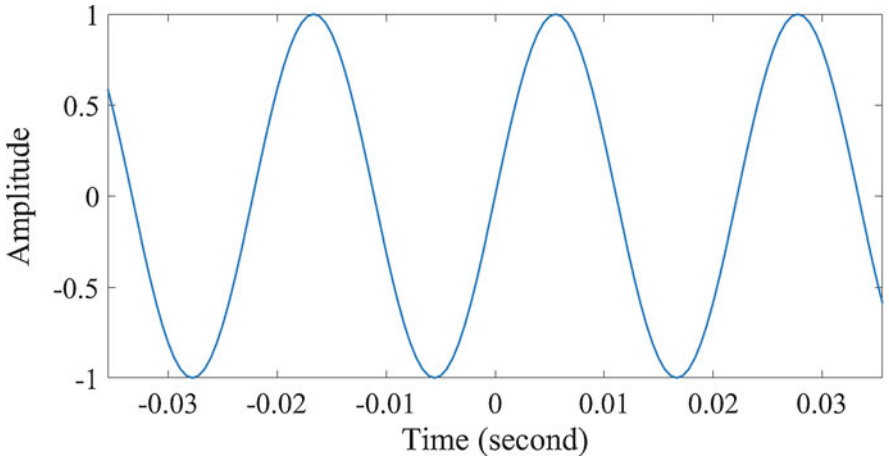

Fig. 12.18 Odd sinusoidal signal

$$x(t) = x(-t) \tag{12.4}$$

On the other hand, odd signals satisfy the following condition:

$$x(t) = -x(-t) \tag{12.5}$$

Figures 12.17 and 12.18 represent the even and odd signals, respectively.

It should be noted that any signal $x(t)$ can be represented in terms of even signal and odd signal.

$$x_{\text{even}}(t) = \frac{x(t) + x(-t)}{2} \tag{12.6}$$

$$x_{\text{odd}}(t) = \frac{x(t) - x(-t)}{2} \tag{12.7}$$

12.3.1.5 Energy and Power Signals

Energy signals have finite energy and the energy of the signal $x(t)$ can be defined as follows:

$$E = \int_{-\infty}^{\infty} x^2(t)dt \tag{12.8}$$

The power signals are those signals which have finite power and the mathematical expression for power can be given as follows:

$$P = \lim_{T\to\infty} \frac{1}{2T} \int_{-T}^{T} x^2(t)dt \tag{12.9}$$

It should be noted that any signal cannot be power and energy signal together and it is also possible that a signal may be neither energy nor power signal.

12.3.2 Types of Systems

Systems are required to process the signals for various applications. There are various types of systems which can be categorized as follows [10]:

12.3.2.1 Linear and Nonlinear Systems

A system which follows homogeneity and additivity principles is known as linear system. On the other hand, a nonlinear system does not follow these principles.

For two input signals $x_1(t)$ and $x_2(t)$, the homogeneity and additivity principles are as follows:

$$L\{a_1x_1(t) + a_2x_2(t)\} = a_1L\{x_1(t)\} + a_2L\{x_2(t)\} = a_1y_1(t) + a_2y_2(t) \tag{12.10}$$

Here, $L\{a_1x_1(t) + a_2x_2(t)\}$ is the overall response of the system and $a_1L\{x_1(t)\} + a_2L\{x_2(t)\}$ represents the individual response of systems of signals $x_1(t)$ and $x_2(t)$, respectively. The overall response of system is equal to the response of

individual systems for a linear system where the sum of these individual responses is not equal to the overall response in a nonlinear system.

Example of a linear system is as follows:

$$y(t) = 7x(t) \tag{12.11}$$

Example of a nonlinear system is as follows:

$$y(t) = x(t) + 7 \tag{12.12}$$

12.3.2.2 Time-Invariant and Time-Variant Systems

A system can be considered as time-invariant if input–output characteristics of the system do not vary with time. On the other hand, a time-variant system does not follow such characteristics.

A system with input signal $x(t)$ and output signal $y(t)$ is time-invariant when

$$L\{x(t-\tau)\} = y(t-\tau) \tag{12.13}$$

where τ is shifting a parameter.

Example of time-invariant system is

$$y(t) = \cos\{x(t)\} \tag{12.14}$$

Example of time-variant system is

$$y(t) = x(3t) \tag{12.15}$$

12.3.2.3 Linear Time-Invariant and Linear Time-Variant Systems

If a system satisfies linear and time-invariant properties, then it is known as linear time-invariant system and a system which satisfies linear and time-variant properties is called a linear time-variant system.

12.3.2.4 Static and Dynamic Systems

A system which does not require memory is known as static system and a system which requires memory is called as dynamic system.

Example for memory-less static system is as follows:

$$y(t) = 3x(t) \tag{12.16}$$

Example of a dynamic system is as follows:

$$y(t) = 3x(t) + x\,(t-3) \tag{12.17}$$

12.3.2.5 Causal and Noncausal Systems

For causal system, the output depends on the present and past values of the input signal. On the other hand, the noncausal system output also depends on the future values of the input signal.

Example of causal system is as follows:

$$y(t) = x(t) + x\,(t-2) \tag{12.18}$$

The following is the example of a noncausal system:

$$y(t) = x\,(t+2) \tag{12.19}$$

12.3.2.6 Invertible and Non-invertible Systems

A system can be considered as an invertible system if the input signal can be obtained on the output signal of the system. When input signal cannot be obtained on the output of the system, then a system is known as non-invertible system.

Example of an invertible system is as follows:

$$y(t) = 3x(t) \tag{12.20}$$

Example for a non-invertible system is as follows:

$$y(t) = 0 \tag{12.21}$$

12.3.2.7 Stable and Unstable Systems

In stable system, bounded input signal provides bounded output signal, whereas in unstable system, we will get unbounded output signal for the bounded input signal.

Example of stable system is given as follows:

$$y(t) = x(t) \tag{12.22}$$

Example of unstable system is as follows:

$$y(t) = \int x(t)dt \tag{12.23}$$

Fig. 12.19 Schematic block diagram of signal acquisition [11]

12.3.3 Signal Acquisition

Signal acquisition is a process in which we study how the physical signals collected from the sensors get into the computers or digitized for the processing of signal in computers and machines. The main blocks of signal acquisition process contain signal conditioning which is mainly possible with a sample and hold circuit and ADC by which a physical analog signal can be converted into a digital signal. The block diagram of signal acquisition process along with sensor and computer interface units is shown in Fig. 12.19. In this Fig. 12.19, sensor senses the physical signal and then signal conditioning is applied with the help of sample and hold circuit, and in order to get this signal in digital domain, an ADC is used. Thus, the converted signal has a number of bits which represent the analog signal at a particular instant of time and which can be stored in a computer with this interfacing mechanism [11].

The typical signal acquisition process has some additional processing units because the sensors have multiple channels. Therefore, a multiplexing unit with sample and hold circuit which quickly scans all the channels and provides data to sample and hold circuit in the short interval of time is required. On the other hand, each ADC has a certain dynamic range of working. The violation of dynamic range of ADC leads to approximation errors during analog to digital conversion process. Thus, it is necessary to amplify the signal to increase the resolution of the ADC. The isolation is also a part of signal acquisition process because the electric and magnetic fields may affect the signal properties. Therefore, a good signal acquisition process should be properly isolated in order to get less interference of external factors. In addition to these abovementioned units, an anti-aliasing filter just after the multiplexer unit is also required because the outputs from the multiplexer are very closely placed in time and the sample and hold circuit with ADC will also take some time to complete the analog to digital conversation process [11].

12.3.4 Time- and Frequency-Domain Representations

The digital signals stored in computer have significant information which enable us to extract the desired information present in the signal. These signals physically exist in time domain and we can analyze the behavior for most of the signals by visual inspection. However, the frequency-domain characterization is equally important for

the analysis of a signal. Therefore, the Fourier transform is a commonly used tool for spectral representation of a time-domain signal. The main motivation behind the uses of different types of transformations in signal processing techniques is due to the fact that transforms can highlight certain characteristics present in signal in different domains.

According to Fourier, a continuous periodic signal $x(t)$ can be formed by combining a number of scaled and phase-shifted sinusoidal components. The frequencies of these components are in multiple of the fundamental frequency (ω_0) for the signal $x(t)$. Hence, the synthesis equation for a general periodic signal $x(t)$ can be written as [12]:

$$x(t) = \sum_{k=0}^{\infty} g_k \cos\left(2\pi k f_0 t + \Psi_k\right) \tag{12.24}$$

where g_k and Ψ_k are sets of constants and $f_0 = \frac{\omega_0}{2\pi}$. Suppose $p_k = g_k \cos(\Psi_k)$ and $q_k = -g_k \sin(\Psi_k)$, then Eq. (12.24) with the help of trigonometric expansion can be written as [12]:

$$x(t) = \sum_{k=0}^{\infty} [p_k \cos(2\pi f_k t) + q_k \sin(2\pi f_k t)] \tag{12.25}$$

Equation (12.25) can also be written as [12]:

$$x(t) = \sum_{k=-\infty}^{\infty} A_k [\cos(\omega_k t) + j.\sin(\omega_k t)] \tag{12.26}$$

where $j = \sqrt{-1}$, $A_k = \frac{p_k \pm j q_k}{2}$, and it is a complex number for $k > 0$ and $k < 0$, respectively. Equation (12.26) with the help of Euler's relation can be written as [12]

$$x(t) = \sum_{k=-\infty}^{\infty} A_k e^{+jk\omega_0 t} \tag{12.27}$$

Here, the magnitude of coefficient, $|A_k| = g_k = \sqrt{\left(p_k^2 + q_k^2\right)}$ and phase $\angle A_k = \Psi_k = \tan^{-1}(q_k/p_k)$. Equation (12.27) is known as Fourier synthesis equation for a periodic continuous signal $x(t)$.

Conversely, the Fourier analysis equation for a periodic continuous signal $x(t)$ with time period T_0 can be written as [12]:

$$A_k = \frac{1}{T_0} \int x(t) e^{-jk\omega_0 t} dt \tag{12.28}$$

It should be noted that k has only integer values and A_k is a discrete function in Eq. (12.28).

Fourier transform is a linear transform which plays a very important role in digital signal processing applications, and fast Fourier transform (FFT) algorithm is commonly used in analyzing the spectral content of any deterministic signal due to less computational complexity.

The discrete Fourier transform (DFT) allows the decomposition of discrete-time signals into sinusoidal components whose frequencies are multiples of a fundamental frequency. The amplitudes and phases of the sinusoidal components can be determined using the DFT and is represented mathematically as [12]

$$X(k) = \frac{1}{N}\sum_{n=0}^{N-1} x(n)e^{-j\left(\frac{2\pi kn}{N}\right)} \tag{12.29}$$

For a given signal $x(n)$ whose sampling period is T with N number of total samples (NT is therefore the total duration of the signal segment). The spectrum $X(k)$ is determined at multiples of fs/N, where fs is the sampling frequency.

On the other hand, the spectrum can also be obtained using Fourier–Bessel series expansion (FBSE) [13–15]. In FBSE, the Bessel functions are used as basis sets for signal representation, and these basis functions are aperiodic and decay over time. These features make FBSE-based representation suitable for analysis of nonstationary signals, while DFT has certain limitations for these kinds of signals. FBSE has been successfully applied for nonstationary and biomedical signals [16–25].

The FBSE of $u(n)$ using zero-order Bessel functions can be expressed as follows [25]:

$$u(n) = \sum_{k=1}^{L} M_k J_0\left(\frac{\beta_k n}{L}\right), n = 0, 1, \ldots, L-1 \tag{12.30}$$

where M_k are FBSE coefficients of $u(n)$ which can expressed as follows [25]:

$$M_k = \frac{2}{L^2(J_1(\beta_k))^2}\sum_{n=0}^{L-1} nu(n)J_0\left(\frac{\beta_k n}{L}\right) \tag{12.31}$$

where $J_0(.)$ and $J_1(.)$ represent zero- and first-order Bessel functions, respectively. The ascending order positive roots of zero-order Bessel function ($J_0(\beta) = 0$) are represented by β_k with $k = 1, 2, \ldots, L$. The order k of the FBSE coefficients is corresponding to continuous-time frequency f_k (Hz) and it can be computed by the expression given as follows [25]:

$$\beta_k \approx \frac{2\pi f_k L}{f_s} \tag{12.32}$$

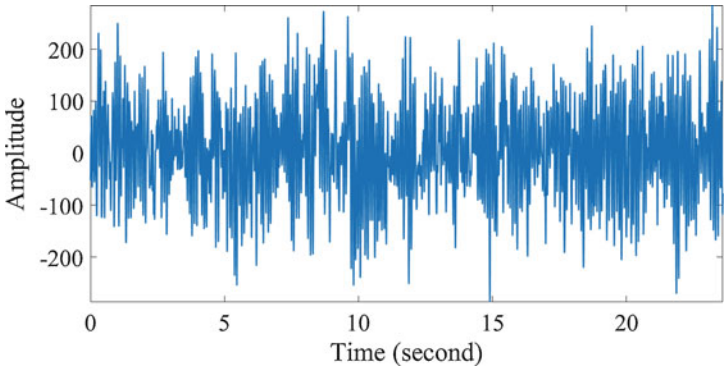

Fig. 12.20 EEG signal of a normal person during eyes-closed condition

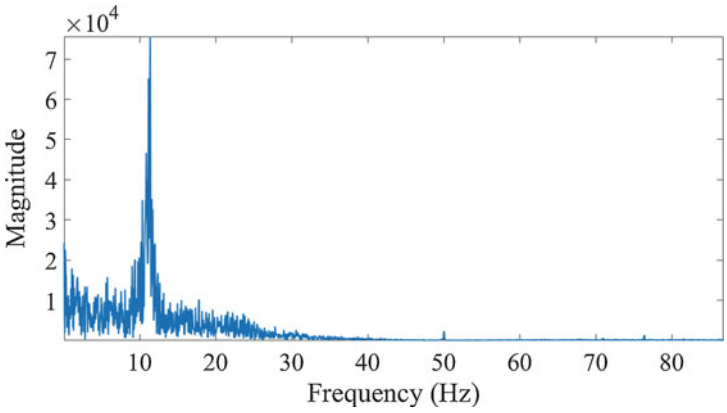

Fig. 12.21 Magnitude spectrum of Fourier transform

where $\beta_k \approx \beta_{k-1} + \pi \approx k\pi$ and f_s is sampling frequency. From Eq. (12.32), the order k can be expressed as follows [25]:

$$k \approx \frac{2 f_k L}{f_s} \tag{12.33}$$

It can be observed from Eq. (12.33) that order k should be varied from 1 to L in order to cover the entire bandwidth of signal $u(n)$. Hence, the magnitude spectrum of FBSE is the plot of magnitude of FBSE coefficients ($|M_k|$) versus frequencies (f_k).

The time- and frequency-domain representations of an eyes-closed normal EEG signal obtained from Bonn University EEG database are shown in Figs. 12.20, 12.21, and 12.22, respectively. The sampling frequency of this EEG signal is 173.61 Hz [26].

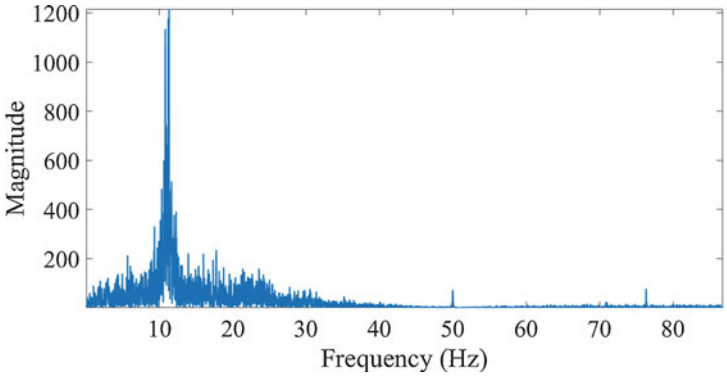

Fig. 12.22 Magnitude spectrum of FBSE

12.3.5 Finite Impulse Response (FIR) and Infinite Impulse Response (IIR) Filters

The response of a FIR filter depends on current and past inputs. Thus, the filter will not produce outputs if it has not received any inputs. The impulse response of this kind of filter is unequal to zero for a finite range. On the other hand, the response of an IIR filter is based on current inputs, past inputs, and past outputs. The dependency of this filter on past outputs generates outputs even after the filter has stopped receiving inputs. The impulse response of an IIR filter is unequal to zero for infinite range. The mathematical forms of FIR and IIR filters for the input signal $x(n)$ and output signal $y(n)$ are as follows [27, 28]:

$$\text{FIR filter}: \quad y(n) = \sum_{i=0}^{M} G_i x\,(n-i) \tag{12.34}$$

$$\text{IIR filter}: \quad y(n) = \sum_{i=0}^{M} G_i x\,(n-i) - \sum_{j=1}^{p} H_j y\,(n-i) \tag{12.35}$$

where G and H are the filter coefficients. The physical structure which will realize Eqs. (12.34) and (12.35) are shown in Figs. 12.23 and 12.24, respectively. In Figs. 12.23 and 12.24, Z^{-1} represents the unit delay element.

The main reason for the description of FIR and IIR filters in this chapter is because the biomedical signals have small amplitude. These signals are contaminated by various artifacts and interferences which change the properties of the signals. One of the commonly present interference in biomedical signals is power line frequency of 50 or 60 Hz. The FIR and IIR filters are used in order to reduce the noise due to power line frequency of 50 or 60 Hz [29].

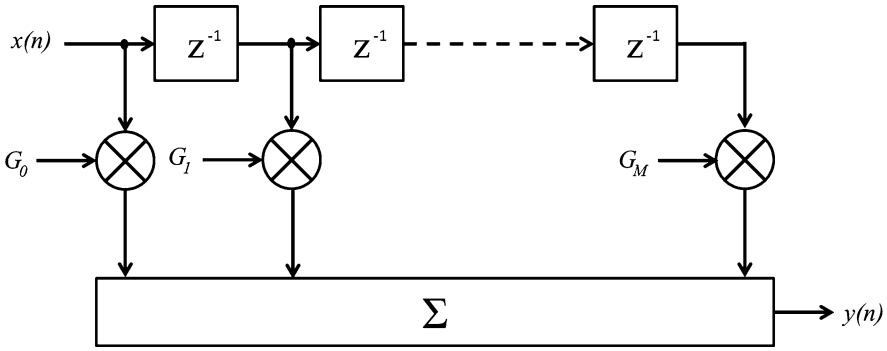

Fig. 12.23 Physical structure of FIR filter [28]

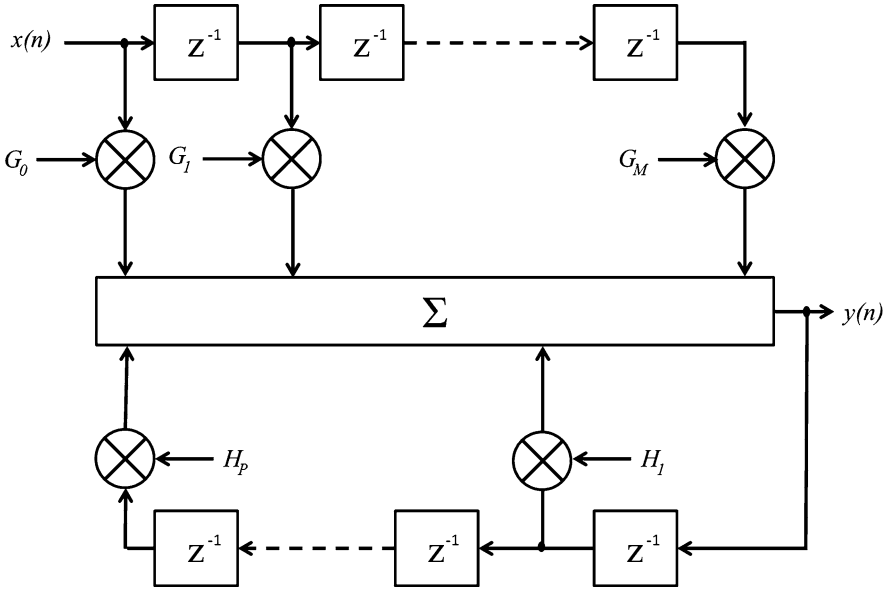

Fig. 12.24 Physical structure of IIR filter [28]

12.4 Types of Biomedical Signals

The electric activities present in the cell which create a potential difference across the cell membrane are used for a number of biomedical signal measurements. These biomedical signals are categorized based on the functioning of different parts of biological system and the descriptions of these biomedical signals are as follows [30].

12.4.1 Electroencephalogram (EEG)

In the biological system, the monitoring and control over the different parts are processed through the brain. The action potentials are used to generate neural activity in the brain and this brain activity can be recorded with the help of electrodes. The signals obtained with these electrodes are known as EEG signals.

The history behind the use of EEG signal is based on an experiment performed in 1929 in which a German psychiatrist named Hans Berger was performing an experiment on his daughter's head to verify the hypothesis that the brain exhibits electrical activity. He observed that the electrical activity increased when she was trying to solve some difficult multiplications. Thus, he deduced from this experiment that the wave patterns observed in the brain recordings reflected the depth of the brain activity [30].

It has been observed that the approximate range of nerve cells in the brain is in the order of 1011. The potential of a nerve cell in steady state is typically around −70 mV, and it is generally negative. On the other hand, the action potential peak is +30 mV and it approximately falls for 1 ms. Thus, the nerve impulse has a peak-to-peak amplitude of approximately 100 mV. In the gray matter, each neuron releases the action potentials during the process of sensing inputs transmitted from other neurons or external stimuli. The spatially weighted sum of all these action potentials at the surface of the skull can be measured by EEG signal. The instrument which is used to record EEG signals is less expensive and accurately measures the brain's electrical activity from the skull. These EEG recordings can be possible in unipolar or bipolar manner. The depolarization signals from the nerve cells may attenuate while passing through the skull because it has complex impedances. Thus, the collections of these signals are possible with quality contact of electrodes with the skull in order to overcome the impedance mismatch created by the hair and dead skin on the skull. The collected EEG signals from the surface of the skull are amplified to represent these signals on electric potential versus time graph [30].

The electric activity in a brain is simultaneously present at many different locations of the head. The most common recording technique of EEG signals utilized 21 electrodes to record these simultaneously occurring electrical activities. The number of these electrodes varies from 64 to 256 for other measuring techniques. The frequency range of amplifiers used to record EEG signals should cover the range from 0.1 to 100 Hz for the analysis of all activities [30].

The EEG signals are broadly used for the diagnosis of various diseases or disorders such as epilepsy, sleep disorders, neurodegenerative diseases, and brain death. The EEG signals of a normal person with eyes-open condition and an epileptic patient during seizure are depicted in Figs. 12.25 and 12.26, respectively [26]. These signals are also obtained from Bonn University database.

The EEG signals are also used in research of brain functional activity. The analysis of evoked potentials (EPs) and event-related potentials (ERPs) of the brain using EEG signal is most common of them. In such applications, the responses of EEG signals are recorded providing specific stimuli such as auditory and visual

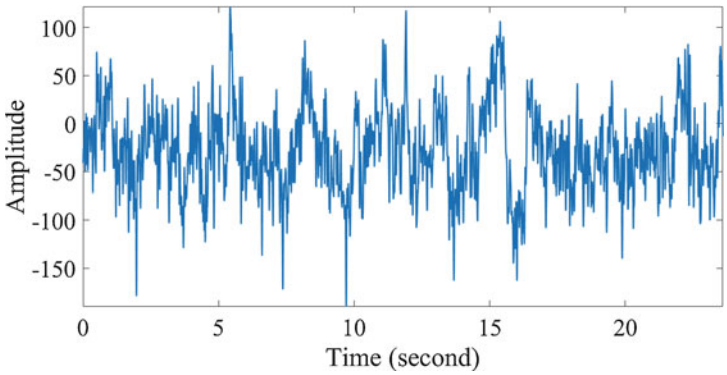

Fig. 12.25 Normal EEG signal with eyes open

Fig. 12.26 Seizure EEG signal from patient

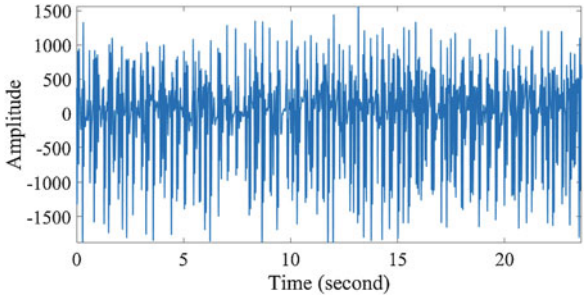

inputs. The EPs and ERPs are particularly used to investigate the response of a brain corresponding to specific stimulation. The level of attention and stress can also be monitored with the help of EPs during experiment.

The major limitation present in EEG signals is that the EEG signals cannot reveal the information about the structure which is responsible for originating these signals. The limitation is due to the fact that the EEG signals are the spatial sum of all action potentials transmitted from billions of neurons at different depths below the cerebral cortex. Therefore, the functional magnetic resonance imaging (fMRI) is used where the functional information from the structures deeply situated in the brain is required [30].

12.4.2 Electrocardiogram (ECG)

The electrical activity recorded from the heart is known as ECG. The ECG signal is used for the clinical diagnosis of heart diseases. The cellular electrical excitation due to cardiac muscle contraction can be recorded by ECG signals. The functioning of these cells can be indicated by its electrical activation, while the depolarization

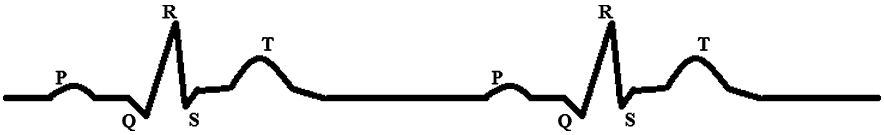

Fig. 12.27 A sample ECG signal with P, Q, R, S, and T wave representation

indicates the shortening of muscle cells. The repolarization and depolarization generate electric potential differences on the muscle cells, which can be recorded using electronic recording instrument. Thus, the ECG signal is due to controlled repetitive electric depolarization and repolarization patterns of the heart muscle cells.

In early history, the ECG signal recording was possible by the efforts of a Dutch scientist Willem Einthoven in 1903. He designed a galvanometer to record the action potentials. The galvanometer was directly coupled to an ink pen. This pen was moved directly on paper as a voltage leading to a deflection of galvanometer was given. Nowadays, the electrodes are directly coupled to amplifiers and filters in order to record ECG signals.

The characterization of ECG signal is usually possible by five waves. These waves are denoted by letters P, Q, R, S, and T. These P, Q, R, S, and T waves can be seen in Fig. 12.27. The ECG signal is also characterized sometimes by a sixth wave with letter U. The P wave in ECG signal is due to depolarization of the atrium, while the Q, R, S, and T waves are caused by the ventricle. The time duration for P wave in ECG signal is approximately for 90 ms and the amplitude for this wave does not usually exceed 2.5×10^{-4} V. During P wave, the atrium contracts to fill the ventricle due to the depolarization. The QRS complex in ECG signal is occurring for time duration of 80 ms with amplitude of about 1 mV. The QRS complex represents the depolarization of the septum and Purkinje fiber conduction. The septum is a wall which separates the left and right ventricle. In simple language, the QRS complex shows the depolarization of ventricular wall from bottom to top and from inside to outside. It should be noted that the quiet time between the P wave and the QRS complex is generally used as a reference line. The repolarization effects of ventricular wall from outside to inside which is also opposite to depolarization represent with a pulse called T wave. During the repolarization process, the atrium is relaxed and filled back. The repolarization process can be distinguished from the depolarization process with the fact that the repolarization process takes longer time as compared to depolarization process. The action potential gradient of the repolarization process is also straightforward wherein it incorporates a smaller gradient in the time derivative of the cell membrane potential. The U wave also shows sometimes a portion of the ventricular repolarization [30].

The ECG signals are used for the diagnosis of various cardiovascular diseases such as myocardial infarction and coronary artery disease (CAD). The ECG signals of a normal person and a patient suffering from CAD are shown in Figs. 12.28 and 12.29. These ECG signals of a normal person and a patient are obtained

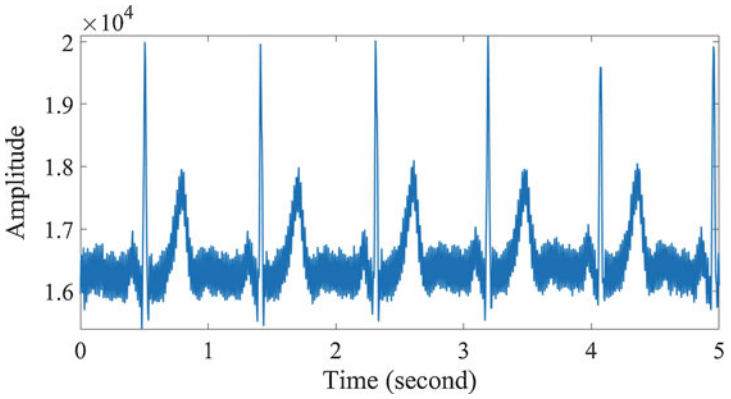

Fig. 12.28 Normal ECG signal

Fig. 12.29 CAD ECG signal

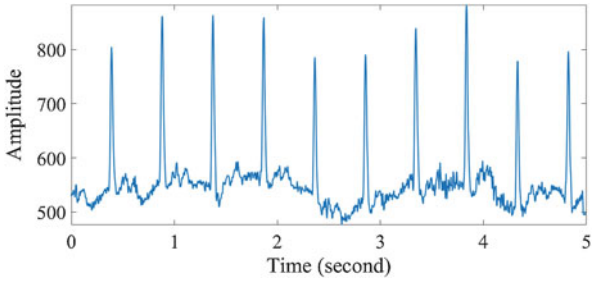

from Fantasia open access database and St. Petersburg Institute of Cardiological Technics 12-lead Arrhythmia Database, respectively [31]. The sampling frequencies of normal and CAD ECG signals are 250 and 257 samples per second, respectively.

12.4.3 Electromyogram (EMG)

The recording of muscle's electrical activities is known as EMG signal. Moreover, the EMG signal is a signal which records the electrical activities produced by the depolarization of muscle cells during muscle contraction. This recording also contains the nerve impulses that initiate the depolarization of the muscle.

In 1907, the first time recording of action potentials produced by human muscle contraction was reported by Hans Piper. The EMG signal has emerged as vital signal in the biomedical field because a number of neuromuscular disorders can be diagnosed using EMG signals.

The recording of the electrical activities of muscle tissue is possible with two methods. In first method, the electrodes are applied on the skin and the signals are recorded from surface of the skin. The second method actually uses the insertion of

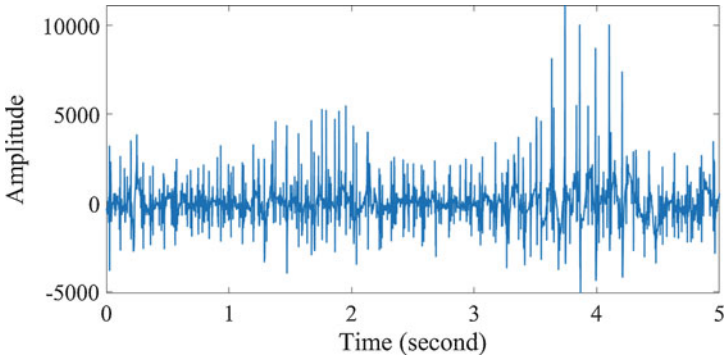

Fig. 12.30 Normal EMG signal

needles with electrodes into the muscle. The EMG signals are the spatially weighted sum of the electrical activities collected from the surface of the skin due to a number of motor units. However, the information present in EMG signal is the combined information of the entire muscle groups. In general, the EMG signal is used to identify the muscle groups which are involved in a particular motion or action.

The EMG signals of specific motor unit can be measured with subcutaneous concentric needle electrodes after implanting it on the muscle. The depolarization of the muscle cells which are present surrounding the needle electrodes can be recorded with these electrodes. Moreover, the electrical activity of a single motor unit can be directly measured with these types of electrodes, and if the needle has more than one electrode, then the bipolar measurement is also possible. There is a short burst activity happening during needle electrode insertion for recording of EMG signals. These burst activities may be repeated several times when an axon of a nerve is touched. The EMG signals also have muscle potential spikes which may be present during muscle contraction. These spikes are not true action potentials of muscle cells because the muscle excitation is usually due to the presence of calcium, potassium, and chlorine ions. Thus, the electrical potential measured from the surface or inside the skin is a triphasic potential phenomenon [30].

The presence of amplitude in excitation potential is sometimes due to the distance between the muscle fibril and the electrode. This amplitude will reduce with the square of distance to the source. The typical range of muscle potential is between 2 and 6 mV with range of time duration of 5–8 ms. The processing of raw EMG signal is performed in a different way as compared to other biomedical signals because these signals often have many noise. The raw EMG signals for a normal person and myopathy patient are shown in Figs. 12.30 and 12.31. These signals are obtained from PhysioBank ATM [31]. The sampling frequency of these signals is 4000 Hz.

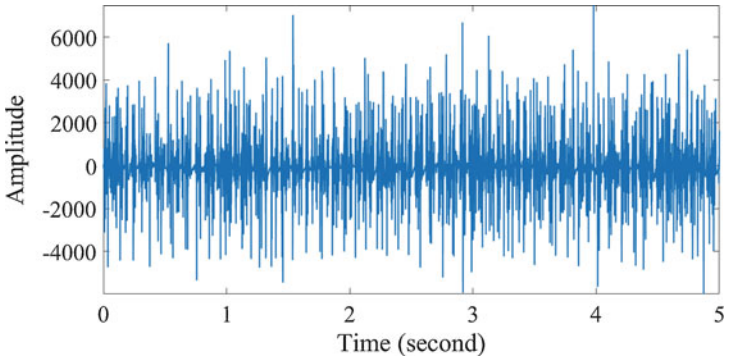

Fig. 12.31 Myopathy EMG signal

12.4.4 Electrooculogram (EOG)

A signal that measures the skin around the eyes is known as EOG signal. The EOG signal is used to determine the gaze and the dynamics of the eye motion. The electrodes used for recording of EOG signals are implanted on the sides of the eyes in order to measure horizontal motions of the eyes. The vertical motions of the eyes are measured with the placement of electrodes above and below the eyes. The motions of the eyes are measured with potential difference between each pair of these electrodes for both cases with the help of differential amplifiers. The presence of this potential difference is due to eyeball movement and it is generated by the cornea and retina. The range of this potential is often between 0.4 and 1.0 mV. The sampling frequency of EOG signal is often in the range of 0–100 Hz and it can be identified by the mechanical limitations of the eye motion.

There are various disorders which can be detected by the EOG signals such as laziness of the eyes in tracking moving objects. In laziness detection, the subject tracks the moving object on a monitor with their eyes and the EOG signals are captured during this event. The diagnosis is based on the lag between the cursor movement and the captured EOG signals.

In another application, the EOG signals help the severely paralyzed patients. In the United States, it is observed that the number of patients who are paralyzed due to spinal injuries is about 150,000. The EOG signals from patients help them to communicate with their caretakers and computers. This communication process requires a large board with an array of commands and placed opposite to the patient.

The gaze angle obtained with EOG signals identifies the command the patient is trying to execute. Similar kinds of systems find importance for navigation of aircrafts and boats.

The EOG signal is very closely related to a signal known as electroretinogram (ERG) signal. This signal is the potential difference among the retina and the eyeball surface. The EOG signal is frequently used to represent ERG signal [30].

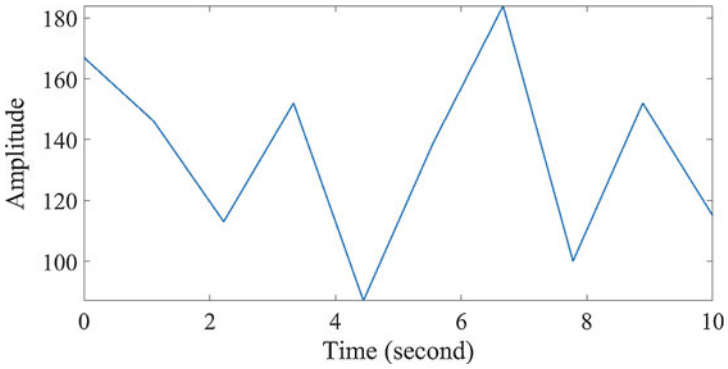

Fig. 12.32 EOG signal recorded with the left eye

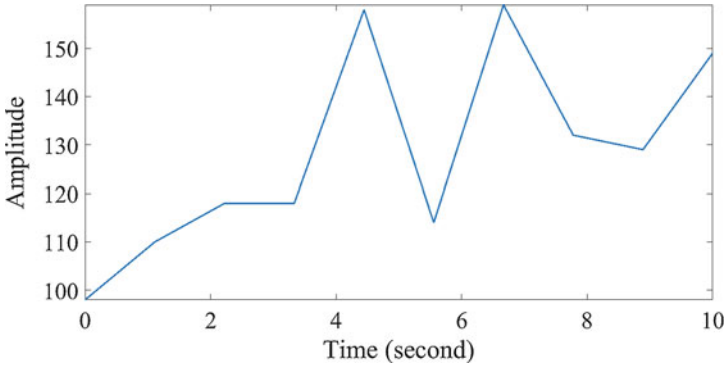

Fig. 12.33 EOG signal recorded with the right eye

The EOG signals of the left and right eyes obtained from PhysioBank ATM are shown in Figs. 12.32 and 12.33, respectively. The sampling frequency of these signals is 1 Hz [31].

12.4.5 Magnetoencephalogram (MEG)

The magnetic field activities of brain neurons are captured by MEG signals. The fact behind the involvement of MEG signal to capture brain activities is based on the electromagnetic theory. The change in electric field causes a magnetic field proportional to electric field. Thus, the change in electric charges of the neurons produces a proportional magnetic field which can be used to measure brain activities. The MEG signal can measure the extracranial magnetic fields created by intraneuronal ionic current flow inside the appropriately oriented cortical pyramidal cells.

The main reason behind the use of MEG signal over EEG signal is that the EEG signals have significant noise because of the muscles' electrical activities being very close to the electrodes, whereas the MEG signal can record from DC to very high frequency (>600) without skin contact. The MEG signal is also capable of detecting neuronal electrical activities from deep inside the brain, while the neuronal electrical activities close to surface of the brain are often captured by EEG signals. Moreover, the MEG signal has less distorted signals which provide much better spatial and temporal representation of the brain. A major advantage of MEG signal is that it can provide an exact location and timing of cortical generators for event-related responses and spontaneous brain oscillations. The MEG signal provides a spatial accuracy of a few millimeters along with submillisecond accurate temporal resolution under optimal conditions. These accurate configurations provide the much effective spatiotemporal tracking of distributed resolution in case of cognitive tasks or epileptic discharges. The weak magnetic field in MEG signal recording machine is sensed by large superconducting quantum interference devices (SQUIDs). The SQUID sensors are able to deliver both natural and evoked physiological responses in MEG signal due to weak strength of magnetic field which is about picotesla (pT). The interference present in MEG signal is mainly due to earth's magnetic field and this interference can be filtered by the MEG signal recording machine. The analysis of MEG signals is possible in a similar way as the EEG signals due to resemblance. Thus, the same processing techniques which are used for EEG signals can be utilized for MEG signals [30].

The MEG signals of left, right, forward, and backward movements from subject S01 are shown in Fig. 12.34, respectively. These signals are obtained from BCI competition IV dataset 3 [32]. The dataset contains ten channels of MEG signals, namely, LC21, LC22, LC23, LC31, LC32, LC41, LC42, RC41, ZC01, and ZC02. These signals are recorded with two subjects S01 and S02 with a sampling frequency of 400 Hz. A total of 400 samples are present in a signal resulting in a 1-s time duration.

12.4.6 Other Biomedical Signals

Biomedical signals are not limited to the abovementioned category of signals. There are many other biomedical signals which are used for clinical and research purpose. The signals which are used for the diagnosis of heart sounds are known as phonocardiogram (PCG) signals. In PCG signals, the heart sounds are observed during the inside and outside flow of the blood in the heart compartments. These signals are often recoded with the help of mechanical stethoscopes which amplify the heart sounds. However, the mechanical stethoscopes have an uneven frequency response and this frequency response distorted the heart sound signals. Thus, an electronic stethoscope can overcome this problem and provide a less distorted heart sound signal.

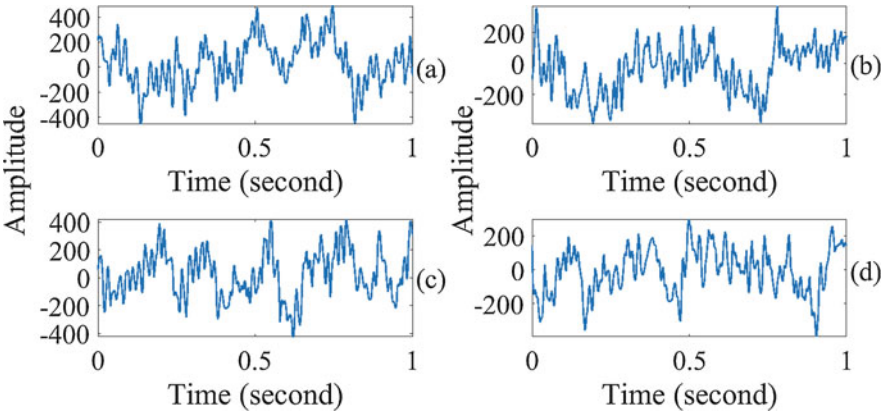

Fig. 12.34 MEG signal of (**a**) left, (**b**) right, (**c**) forward, and (**d**) backward movements recoded with LC21 electrode from S01 subject

A typical application of PCG signals is to detect heart murmurs. In murmurs, the heart sounds are usually due to imperfections in the heart valves or the heart walls. These murmurs are also present in infants due to flow of blood from one side to the other side of the heart through a hole. This hole in infants is usually filled in a few weeks after birth which will stop the heart murmur.

Another signal which records the electrical activity of the stomach is known as electrogastrogram (EGG) signal. The midcorpus of the stomach generates this electrical activity with intervals of approximately equal to 20 s in humans. This signal consists the rhythmic waves of depolarization and repolarization of stomach muscle cells. These waves are related to the spatial and temporal organization of gastric contractions. The external (cutaneous) electrodes can record the EGG signal [33].

12.5 Physiological Phenomena and Biomedical Signals

The biomedical signals can also represent the physiological phenomenon. Hence, the physiological parameters can be reflected by biomedical signal parameters. These biomedical signal parameters can be obtained with an adequate knowledge of their physiological causes for diagnosis purpose. Figure 12.35 shows a block diagram approach to extract physiological parameters from recorded biomedical signals. These parameters are extracted using signal processing techniques and the radically different biomedical signals may have information of the same physiological parameter (heart rate, respiratory rate, etc.) [34].

Fig. 12.35 Block diagram for physiological parameter extraction process [34]

12.5.1 Vital Phenomena and Their Parameters

There are various physiological phenomena as well as biomedical signals. Therefore, we focus on some of the vital phenomena which are frequently used in clinical practice such as heartbeat, blood circulation, blood oxygenation, and body temperature. A brief description of these phenomena is given as follows [34].

12.5.1.1 Heartbeat

The heart is used for pumping blood into the circulatory system using its rhythmic contractions which create pulsating waves of blood pressure and blood flow. The cardiac cycle obtained with this heart rate is very important for diagnosis purpose [34].

There are three widely used methods to register this cardiac activity. In the first method, the ECG signal is used to show the rhythmic waves and peaks which are corresponding to heart muscle excitation with heart rate. An optical biomedical signal named as optoplethysmogram (OPG) is used in the second method to represent a smoother waveform reflecting pulsating blood absorption of incident light. In the third method, the PCG signal represents two consecutive temporary signal deflections corresponding to heart sounds which are induced by consecutive closures of heart valves. The cardiac activity recorded with the ECG signal has nearly instant response at the corresponding sensor location, while the time delayed response is observed in the recording of OPG and PCG signals due to the pulse wave propagation velocity and sound velocity, respectively [34].

Although the spontaneous cardiac activity is inherently present in many pacemaker tissues of the heart, the heart rate level and its change are mostly controlled by the autonomic nervous system. This control is possible with the sinoatrial node, which is the main pacemaker in the heart. The activities of sympathetic and parasympathetic nervous systems directed to the sinoatrial node are characterized by discharges synchronous with each cardiac cycle. These activities can be modulated with central oscillators present in the central nervous system and peripheral oscillators which depend on respiratory movements and arterial pressure fluctuations. The balance between these activities determines the instantaneous heart rate. The central and peripheral oscillators create noisy fluctuations in the corresponding instantaneous heart rate. However, these types of fluctuations can also be observed at different timescales [34].

The estimation of energy expenditure in the body is the most efficient measure which can be calculated with the help of the heart rate level because heart rate

increases with increase in oxygen consumption at an instant. The heart period which is a reciprocal of heartbeat is generally referred to as RR interval (the time interval between two consecutive R peaks in ECG signal). The only criterion for considering the RR interval is that the sampling frequency should be very high (>500 Hz) to assess the sinoatrial node activities.

The heart rate variability (HRV) is another standard term which describes heart period oscillation as well as the oscillation between consecutive instantaneous values of heart rate. The HRV is very closely related to the mechanism of the autonomic nervous system which gives immediate response to any physiological states such as respiration phase, sleep stages, and emotional activities. The HRV is also good in representing functional integrity of a physiological process (thermal, hormonal, neural, etc.) Therefore, the assessment of HRV gives early signs of pathological developments such as cardiovascular diseases [34].

12.5.1.2 Respiration

In the respiration process, the lung plays a major role which delivers oxygen to the bloodstream and releases carbon dioxide from the blood through a rhythmic expansion and contraction process. The assessment of respiratory cycle performs an important role in the diagnosis of various diseases. There are numerous methods to register the respiration on which the three well-established methods are discussed here [34].

In the first method, the mechanorespirogram signal is a mechanical biomedical signal used to record the circumference changes of the abdomen and chest during breathing. A periodic waveform showing respiratory rate is observed through this process during normal breathing. On the other hand, this waveform disappears during holding of breath. The amplitude deflection in this signal increases during snoring in order to overcome an increased respiratory resistance. The recorded mechanorespirogram signal from the abdomen and chest may differ in amplitude and phase due to different strengths of abdominal and chest breathing. The waveform recorded from abdominal breathing is delayed with respect to the waveform recorded with chest during breathing [34].

The lung sounds are also present in PCG signal during normal breathing due to air turbulences in the lung branching airways. These sounds have much lower amplitude; due to this reason, it cannot be easily distinguished over time. In addition, an overlapping signal component is also recognizable during the inspiration phase of snoring sounds. This signal component is present due to elastic oscillations of the pharyngeal walls which may lead to a temporal closure of the airways [34].

In the third method, a mechanical biomedical signal is used which records the airflow through the mouth considering nasal airflow is stopped using a tube with a woven screen inside which acts as a flow resistance. This method is commonly used in clinical practice. In this method, the airflow is considered positive and negative corresponding to inspiration and expiration during normal breathing, respectively. The flow is zero during holding of breath. The high-frequency oscillations of the

flow can be obtained during inspiratory phase of snoring. The amplitude of flow is also increased during the phase of both inspiration and expiration of snoring. These oscillations and increased amplitude of flow are due to intermittent closures of the airways and the aforementioned intensified respiratory efforts [34].

In addition to these methods, the thermal biomedical signal is known as thermorespirogram signal in which variations of the air temperature are observed in front of the nostrils during breathing. The temperature increases during expiration and decreases during inspiration phases of breathing. The registration of the respiratory activity is also possible with an electric signal known as electroplethysmogram signal. In this method, the inflated and deflated lung changes the thoracic electrical impedance which can be observed by electroplethysmogram signal. The optical biomedical signal known as optoplethysmogram signal can also be used to register the respiration activities. This signal reflects the peripheral blood volume changes over the respiratory cycle [34].

During respiration, the breath-holding condition deserves some extended description. This condition is generally known as a Greek word apnea (breathlessness) in which a complete or partial cessation of effective respiration occurs. This breath-holding condition can also be possible during sleep at night and it is known as sleep apnea. The sleep apnea is usually detected by polysomnography [34].

12.5.1.3 Blood Circulation

The blood circulation mainly depends on systemic and pulmonary circulation in which the first one comprises the rhythmic transport of the oxygenated blood to the body and the deoxygenated blood back to the heart, whereas the second one is used for the transportation of the deoxygenated blood to the lungs and oxygenated blood back to the heart. In addition to assessment of cardiac cycle with heart rate, a simultaneous registration of blood circulation is also required for the highly relevant diagnosis purpose with the help of circulatory parameters, namely, blood pressure, blood flow, and arterial radius. The brief description for the registration of these circulatory parameters is as follows [34].

Blood Pressure

The unobtrusive and long-term monitoring is difficult in blood pressure registration. The characteristics such as systolic value, diastolic value, and the pressure pulse waveform are used to assess the blood pressure. There are basically some invasive and direct methods as well as noninvasive and indirect methods to register the artifacts of free blood pressure values [34].

In invasive and direct methods, the blood pressure is directly recorded in the vessel by inserting a catheter with a mounted internal pressure sensor or a fluid-filled and rigid catheter for transmitting the blood pressure characteristics to the

external pressure sensor. Although these methods are precise and direct, they are not popular due to their invasiveness and related complications for routine use. On the other hand, the noninvasive methods are popular for the determination of blood pressure characteristics. These methods include the auscultatory method, oscillometric method, volume clamp method, and tonometric method [34].

In auscultatory method, the Korotkoff sounds are detected by a stethoscope to determine systolic and diastolic values. In this method, an inflatable cuff encircles an extremity (upper arm) and the cuff pressure is increased until a complete cessation of downstream blood circulation is observed. The first release of the cuff pressure after cessation resulted in the Korotkoff sound which indicates the time instant when the upper (systolic) part of the blood pressure pulse wave passes under the cuff and the cuff pressure is equal to systolic value. On the other hand, the transition from muffling to silence indicates the time instant when the lower (diastolic) part of the pulse wave passes and at this time instant the cuff pressure is equal to diastolic value [34].

The second method is the successor of the ancient mercury sphygmomanometer. It is based on the principle that the pulsatile blood flow generates radial oscillations of the arterial vessel wall. These radial oscillations are transmitted to the cuff encircling an extremity and then to a pressure sensor kept inside it. During the deflation, the intra-arterial blood pressure exceeds the cuff pressure and the oscillations of the vessel walls are strengthened due to turbulent flow of blood and progressing arterial decompression. The cuff pressure during the initial increase in oscillation amplitude is proportional to the systolic value and the diastolic value is proportional to cuff pressure value at the time of subsequent rapid decrease in the oscillations. In this method, the maximal amplitude of the oscillations for the vessel walls and cuff pressure is obtained when the cuff pressure passes the mean arterial pressure [34].

The volume clamp method is another noninvasive method in which a miniaturized cuff fixes on a finger. This cuff is equipped with as optical transmission sensor. This method is based on the principle that the radius (volume) of the finger artery tends to increase at the time of the blood pressure (volume) pulse and this increased radius is detected by transmitted light intensity. Afterward, the cuff pressure (volume) is increased just enough to keep the radius and transmural pressure constant. The resulting cuff pressure is proportional to blood pressure waveform because the cuff pressure follows the intra-arterial pressure up to a constant factor at constant transmural pressure. A pneumatic feedback system is also used in this method for cuff pressure (volume) control so that a maximum pulsatile change of the vessel radius is achieved when transmural pressure approaches zero. The cuff pressure pulsations roughly equal to intra-arterial pressure at the time of zero transmural pressure. The main advantage of this method is that it does not require previous calibration with patients to attain absolute blood pressure values [34].

The last one method is the tonometric method which is a successor of the ancient sphygmograph. In this method, a rounded probe over a superficial (radial or carotid) artery which has a backside support of bone is pressed, allowing the artery to be

flattened in a reproducible way. The flattening removes the tangential forces in the arterial wall and the rounded probe is barely exposed to the artery pressure. During flattened artery, the applied force by the rounded probe is opposite and equal to the pulsatile force. This force exerts in such way that the pressure of blood exerts on the flattened arterial wall. This rounded probe is connected to a pressure sensor which reflects waveform of blood pressure. This method requires an initial calibration with the patient to compensate changes of arterial mechano-elastic function among patients in order to obtain absolute blood pressure values [34].

Blood Flow

The recording way of blood flow is analogous to blood pressure. The blood flow can also be recorded in invasive and noninvasive ways. The stroke volume, blood flow velocity, and pulsatile flow waveform are the parameters of interest in blood flow registration [34].

The invasive methods for blood flow monitoring have fewer acceptances due to invasiveness and related complications. Some of the invasive methods are indicator method, electromagnetic method, and transit-time ultrasonic method [34].

In indicator method, the oxygen is used as an indicator which is introduced into the stream of blood flow and the resulting arterial as well as venous concentrations from this indicator are measured based on Fick principle. Alternatively, a thermistor catheter is used to introduce a bolus of ice-cold saline into the right atrium. This catheter is also used to detect the resulting drop in temperature of the blood which is present in the pulmonary artery. The amount of indicator injected divided by the area under the blood temperature dilution curve represents the cardiac output in this method. In the second method, the blood vessel with flowing blood is exposed to electromagnetism. The blood vessel is placed in transverse magnetic field which induced a potential difference in the blood vessel with flowing blood. This potential difference is directly proportional to internal diameter of the vessel and the mean blood flow velocity which can be used to measure the blood flow. In the last transit-time ultrasonic method, an ultrasound beam (wave) passes through the blood vessel. There are two ultrasound receivers placed diagonally on either side of the vessel. The difference of time taken for the ultrasound to pass in one direction as opposed to the other is used to obtain waveform for the flow velocity of blood [34].

The noninvasive methods for the determination of blood flow parameters are frequently acceptable. There are many methods for the noninvasive registration of blood flow from which three of the most popular are echocardiographic method, impedance cardiography method, and pressure pulse contour method [34].

The echocardiographic method is based on ultrasonic Doppler effect. In this method, an ultrasound beam in the frequency range of a few MHz is backscattered from the moving blood cells. The blood velocity is related to frequency shift due to backscattered sound. In other words, the frequency increases when the blood moves toward the ultrasound probe. The volumetric blood flow can be computed from the velocity profile over the cross-sectional area of the vessel combined with

the cross-sectional dimensions. In impedance cardiography method, an electric current is introduced and the resulting voltage is measured across the axial direction of the thorax while most of electric current follows the path of least resistance and seeks the path of blood-filled aorta. The thoracic impedance is represented by measured voltage. During the cardiac cycle, the volumetric changes of the aorta induced thoracic impedance changes allowing for the determination of the cardiac stroke volume in absolute units. This method is also known as electric field plethysmography. In another pressure pulse contour method for blood flow registration, a generalized transfer function is used to derive the aortic pressure from the radial pressure and then the aortic flow obtained with applying an aortic impedance model. This model indicates the ratio of aortic pressure and flow. During a cardiac cycle, the stroke volume is the integral of the flow waveform. This method requires a previous calibration to achieve absolute blood flow values [34].

Arterial Radius

The mean value of the arterial radius and its pulsatile waveform are interesting topic in physiological phenomena. There are various invasive and noninvasive methods for the monitoring of arterial radius like blood pressure and blood flow. The methods used to calculate arterial radius are somewhat similar which are used for blood pressure measurement. However, the measurement of arterial radius is more sensitive than that of blood pressure measurement due to the reason that the radius changes up to 10%, while blood pressure may change up to 50% [34].

The invasive methods for the measurement of arterial radius are based on resistance/inductive strain gauges, photoelectric devices, and transit-time ultrasonic approach [34].

In the first method, the resistance/inductive strain gauges are fixed directly to the outer artery wall or even inserted into the artery in order to measure radius by the catheter. The second method is based on photoelectric devices in which a pulsating artery casts a shadow on a photocell. The transit-time ultrasonic approach is similarly used like those for blood flow registration. In this method, the two ultrasound transceivers are placed opposite to each other on the outer sides of the arterial wall. The time taken between the impulse emission and its reception on the opposite side is proportional to the arterial radius [34].

The most popular noninvasive methods for the registration of arterial radius are based on ultrasonic beams, optical plethysmography, and mechanical plethysmography [34].

In ultrasonic beam method, the reflections of the ultrasound waves are used and the time taken between the impulse emission from the ultrasound probe on the skin and reflected impulse reception from both arterial walls is calculated, which delivered the arterial radius. The method based on optical plethysmography is an indirect method to assess the local pulsatile volume of the transilluminated artery. In this method, the arterial radius increases with each blood pulse and the transilluminated region encloses with an increased ratio of blood which strongly

absorbs the incident light as compared to the surrounding tissue. As a consequence, the intensity of transmitted light decreases for increased arterial radius or at the time of systole. This method not only assesses the pulsatile changes of the local blood volume but also assesses the basic level of blood absorption related to blood oxygenation. The recorded biomedical signal shows similarity with blood pressure from the carotid artery and mild similarity with blood pressure recorded with the ascending aorta but no similarity is obtained with the radial artery blood pressure. Another method is based on mechanical plethysmography which targets local skin curvature in order to assess a superficial artery such as the carotid artery on the neck. During arterial cardiac deflections, the curvature of the local skin changes and it can be assessed by a skin curvature sensor [34].

12.5.1.4 Blood Oxygenation

Blood circulation implies a rhythmic transportation of oxygenated and deoxygenated blood from the lung and back to the lung. Hence, the blood oxygenation level is a vital physiological parameter which is usually extracted with optical biomedical signals. In this method, the light absorption due to pulsatile arterial blood is measured at two wavelengths and interrelated by an algorithm. The blood oxygenation level is usually maintained at a fairly constant level. Thus, the monitoring of blood oxygenation level is very important in order to diagnose cardiac and vascular anomalies. This examination is more specific for anesthesiology to prevent an inadequate oxygen supply. The presence of oxygen in arterial blood is due to binding of oxygen molecules with hemoglobin and dissolving of oxygen with blood plasma in gaseous state. However, the quantity of oxygen in the blood is mainly due to hemoglobin oxygenation as blood plasma carries a very less amount of oxygen. Therefore, the oxygenated hemoglobin implies as a local oxygen buffer to maintain the partial pressure of oxygen in the plasma. On the other hand, the reduced hemoglobin reserves oxygen in the pulmonary capillaries by depleting partial pressure of oxygen in the plasma, resulting in oxygenated hemoglobin. Although blood plasma contains a negligible amount of oxygen, it plays an important role in delivering oxygen to the tissues and the storing of oxygen in the pulmonary capillaries by hemoglobin. It should be noted that the noninvasive assessment of blood oxygen level in the elderly is faced with progressing accuracy problems by optical method [34].

12.5.1.5 Body Temperature

The temperature of the human body is generally governed by the heat production and loss. During rest condition, the heat production is usually carried out by the inner organs such as kidneys, liver, heart, intestines, and brain under the scope of metabolic activity. The rest condition in metabolic activity generally consumes almost 50–70% of daily energy. During normal condition, the inner organs produce

more than 50% of thermal energy and about 20% by the skin and muscles, whereas the contribution of the skin and muscles may reach to 90% during physical work [34].

On the other hand, the heat loss is represented by heat radiation, heat convection, and evaporation. The heat radiation and evaporation are proved more powerful at room temperature and warm environment. The heat loss cannot be efficiently realized by the proximal skin surface because its shape is too flat for efficient heat transfer to the environment. Hence, the heat loss mostly occurs from distal body parts such as fingers and toes which have high surface to volume ratio in order to conduct heat to the environment. In other words, the body consists of a heat-producing core which regulates the temperature at 37 °C homeostatically. The core body temperature reflects a circadian variation of about ±0.6 °C with a maximum in the early evening nearly around 6 p.m. and a minimum during 3 a.m. The regulating mechanisms involve a readjustment of the target temperature value of 37 °C during the whole day. This target value is instructed by the central nervous system of the brain (hypothalamus region), while the actual value registration of core body temperature by the thermal receptors is also carried out in hypothalamus region [34].

12.5.2 Parameter Behavior

The vital physiological phenomena of the heartbeat, respiration, blood circulation, blood oxygenation, and body temperature represent specific changes in their reflexive and tonic behavior. The typical behavior and interrelations of the physiological parameters are also a major concern in order to coordinate and integrate body functions. The physiological parameter behavior with their mutual coordination facilitates vital physiological functions, limited resources of body energy, limited space and time in organs and cells for life-supporting functions, environmental changes adaptation, adaptation to physical and mental stress, and regeneration task of the body with sleep [34].

The behavior and coordination of the physiological parameters can be explained with a feedback control loop represented in Fig. 12.36. The hypothesis behind the control loop is that the central nervous controls the physiological phenomenon or function through a quantitative feedback such as thermal, chemical, and pressure receptors. The desired performance can be obtained by minimizing the error calculated with the difference between the target and actual value of the physiological parameters. In this way, controlled body functions can be achieved with the help of the central nervous system. In Fig. 12.36, the controller comprises neurogenic, myogenic, and hormonal controls. The neurogenic control yields a fast response with the help of the autonomic nervous system while as myogenic control through muscle excitation. The slow response is obtained with hormonal control with the release of hormones [34].

The cardiovascular system is an example of this feedback control system in which when blood pressure drops below the normal value, the arterial stretch-

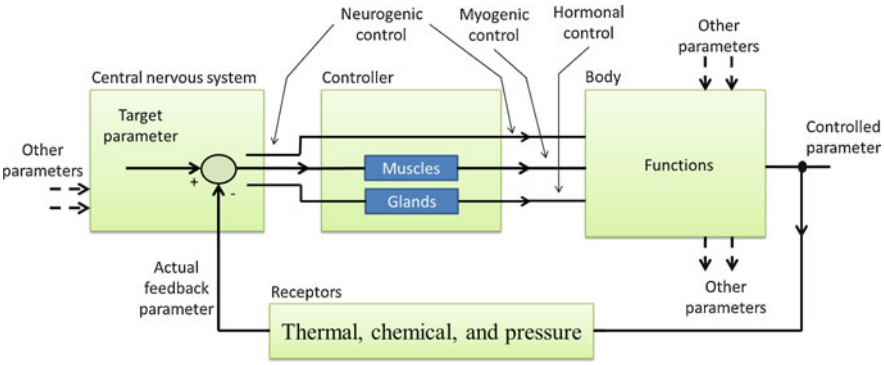

Fig. 12.36 Feedback control loop of the physiological parameters [34]

sensitive receptors (baroreceptors) give an imbalance signal of blood pressure to the brain. The difference of the actual and target values of the blood pressure starts neurogenic control inhibiting the vagus nerve parasympathetic activity which is connected to the sinoatrial node (pacemaker) of the heart. Afterward, the heart rate and contractility of the heart muscles increased. In parallel to this activity, myogenic control forces are applied to increase the total peripheral resistance through smooth muscle activation in the peripheral arteries and increase in regulatory action normalizing the blood pressure level [34].

Mutual interrelations of physiological functions and parameters are basically depending on control loops. In particular, physiological parameter interrelations are needed for the efficient use of energy in humans. The main interrelations of the physiological phenomena during inspiration are cardiorespiratory and cardiovascular interrelations [34].

In cardiorespiratory interrelations, an increase in the inspired air volume resulted in decrease in the left ventricular stroke volume as well as increase in heart rate to level off the cardiac output; due to this efficient blood supply is achieved [34].

In cardiovascular interrelations, a decrease in the systolic blood pressure overlapped with an increase in heart rate to level of the blood pressure [34].

The cardiorespiratory and cardiovascular interrelations are driven by a complex interaction of the circulatory and pulmonary systems with the hemodynamic and nervous systems [34].

In addition, a phenomenon known as biological rhythms which is a periodic and cyclic phenomena of living organs and organisms is described in order to explain the fact that organism needs to give a special performance as well as operating efficiency should be assured by regeneration. These rhythms are used to integrate and coordinate body functions. These rhythms can also be used to anticipate environmental rhythms around the body. This can help to reduce energy due to tuning and synchronization of rhythms, especially during rest or sleep. The exogenous and endogenous are the two types of biological rhythms. In exogenous rhythms, the rhythms are directly controlled by the environment around the body

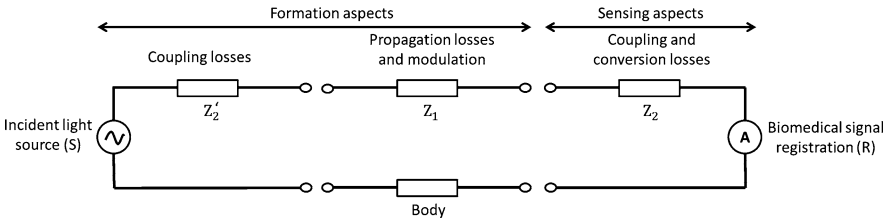

Fig. 12.37 Electrical model for the registration of induced optic biomedical signal [35]

such as the presence of light. On the other hand, the internal biological clocks drive the endogenous rhythms [34].

12.6 Sensing by Optic Biomedical Signals

The optic biomedical signals are induced biomedical signals in which an artificial light source is coupled to biological tissue. This source resulted in a transmitted light intensity which is strongly governed by the light absorption and scattering phenomenon in the biological tissue. The induced optic biomedical signal due to this phenomenon is proportional to the light absorption strength and is usually registered for diagnosis purpose such as blood oxygenation and blood volume. Consequently, the transmitted light intensity also shows multiple physiological parameters which are very useful for the assessment of the health state [35].

The optic biomedical signals are traditionally used to register blood oxygenation and heart rate. The recent advancement in medical technology has also the waveform analysis of optic biomedical signals which facilitate the derivation of respiratory rate. The state of vascular structures (arteries and veins) can also be indicated by the waveform of optic biomedical signals [35].

The model for the understanding of formation and sensing aspects of optic biomedical signals can be seen in Fig. 12.37. In Fig. 12.37, the incident artificial light source is represented by voltage source S which is applied on the skin and coupled to body tissue. The coupling losses are represented by electrical impedance $Z_2{}'$. The propagation of the coupled light throughout tissue modulated by diverse physiological phenomena and the electrical impedance for modulation is Z_1. Consequently, some light portion leaves the body and it is available for the detection purpose over the skin. This light is coupled with light sink at a certain distance from the light source in which coupling losses are represented by electrical impedance Z_2. Afterward, the transmitted light intensity is converted into an electric signal which resulted in registration of optic biomedical signals [35].

12.6.1 Formation Aspects

The formation aspects basically revealed the propagation light modulation in body tissues simultaneously with dynamic physiological phenomena. This modulation extracts the physiological information present in optic biomedical signals. The formation aspects of the induced optic biomedical signal include an artificial incident light source which entered the body through the skin, incident light coupling into body, and light propagation through body tissues to a distant light sink applied on the skin [35].

The emission of the artificial incident light depends on the accelerated charge in which energy is released during the transition of electrons from higher to lower energy levels resulting in light emission. The sources of light used for this purpose are of two types, namely, broadband and narrowband. The broadband light sources emit light in a relatively wide band of the electromagnetic spectrum such as incandescent lamps and noble gas arc lamps whereas a narrowband is covered by narrowband light sources such as lasers, fluorescent sources, and light-emitting diode (LED) [35].

In these light sources, the LED is the most popular and widely used light source in order to induce optic biomedical signals. The LED basically works on the principle of electroluminescence. A charge migration takes place to obtain the light photon [35].

After coupling of light source, the transmission of light through biological tissue is a major aspect. The optical light path is started with the light source and then it diffuses through tissue. The diffusion is subjected to changes in light intensity because of the light absorption, diffraction, reflection, scattering, and refraction. A large portion of light intensity has also dissipated and does not reach the skin where a light sink is placed due to this fact [35].

The interaction between light and tissue can be determined quantitatively such as quantitative strength and duration of the interaction and the spatial distribution of the tissue interaction. The interaction is limited to areas of tissue where coupled light is easily reached. This interaction depends on light and tissue characteristics in which light characteristics represent size of incident light, while light transmission is determined by tissue characteristics [35].

The propagation velocity (υ) of light in a biological medium which oscillates with frequency (f) and wavelength (λ) along its propagation path can be written as [35]:

$$\upsilon = \lambda \times f \tag{12.36}$$

where the electric and magnetic properties of propagation medium determine the value of υ and it can be computed as follows [35]:

$$\upsilon = \frac{c}{\sqrt{\mu_r \varepsilon_r}} \tag{12.37}$$

Here, c is the speed of light in vacuum ($c = 3 \times 10^8$ meter/second), μ_r is the relative magnetic permeability ($\mu_r \approx 1$ in biological media), and ε_r is the relative electric permittivity ($\varepsilon_r \gg 1$ in biological media).

The light energy (photon energy) can also exist and it can be given as follows [35]:

$$W = \frac{h \times \upsilon}{\lambda} \tag{12.38}$$

Here, W is the photon energy and h is Plank's constant ($h = 6.6 \times 10^{-34}$ Joule second).

The induced light is subjected to volume and inhomogeneity effects. In volume effects, the light absorption takes place which attenuates the propagation of light beam in homogenous medium. On the other hand, the heterogeneous medium causes scattering, diffraction, reflection, and refraction effects which attenuate and redirect the light beam in a particular direction in inhomogeneity effects. These effects are not fully independent to each other [35]. The basic inhomogeneity effects are shown in Fig. 12.38 [36]. In Fig. 12.38, the reflection of light occurs at biological tissue interface and the refraction of light occurs when the light enters in tissue that has different refractive index. The absorption and scattering of light also take place in between the tissue structure. The physical parameters such as refractive index, absorption coefficients, and scattering coefficients related to these inhomogeneity effects vary continuously at biological tissue boundaries. The different biological tissues have different strengths of absorption coefficients which determine penetration power and energy absorption into a specific tissue from a particular light source. The absorption degree is depending on the type of tissue and wavelength of light in many cases. The mainly light absorption takes place between the wavelength range of UV (<400 nm) and IR (>2 μm). Hence, the light cannot deeply penetrate in this spectral range and attenuation due to scattering is less in this range. The scattering causes broadening of light beams and the light beams decay as it travels through the tissue due to this scattering phenomenon. This scattering phenomenon dominates over absorption in the spectral range of 600–1600 nm and the forward and backward scattering of incident light within tissue are used in various optic biomedical applications such as Raman vibrational spectroscopy and surface-enhanced Raman scattering (SERS) [36].

The reflection and transmitted modes of light can also be used for various optic biomedical applications such as optical plethysmography. The different arrangements of light source and sink are used for reflection and transmitted modes of operation. Figures 12.39 and 12.40 show the different arrangements of light source and sink for reflection and transmitted modes of operation applied on a finger, respectively. In reflection mode, red and near-IR lights are generally used due to the fact that these lights can penetrate tissue to relatively large depths as compared to other lights. The arrangement of light source and sink for red and near-IR lights are shown in Fig. 12.41. In Fig. 12.41, the light source and sink for red and near-IR lights are arranged in reflection mode which yields different pathways by photons

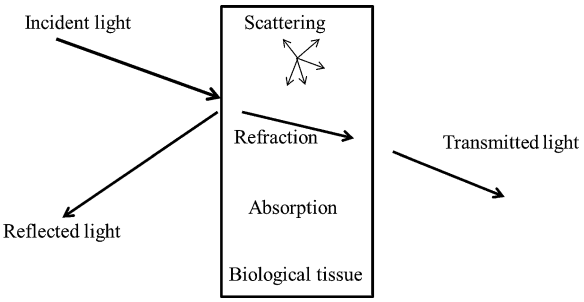

Fig. 12.38 Inhomogeneity effects [36]

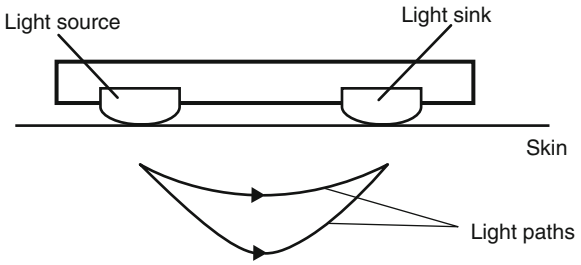

Fig. 12.39 Reflection mode [35]

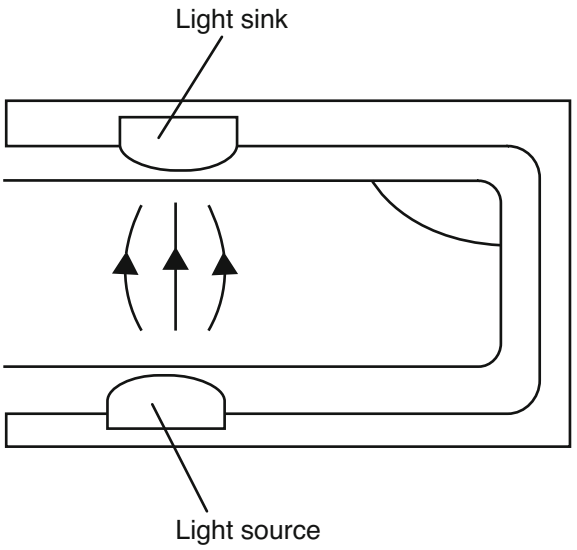

Fig. 12.40 Transmitted mode [35]

of both wavelengths and these paths vary with hemoglobin oxygen saturation which is denoted by S [35].

The light is also dynamically modulated by physiological phenomena in tissue due to the reason that a physiological phenomenon modulates optical properties of the tissue. There are various light absorbers present in tissue such as pulsatile arterial blood, nonpulsatile arterial blood, capillary blood, venous blood, bloodless

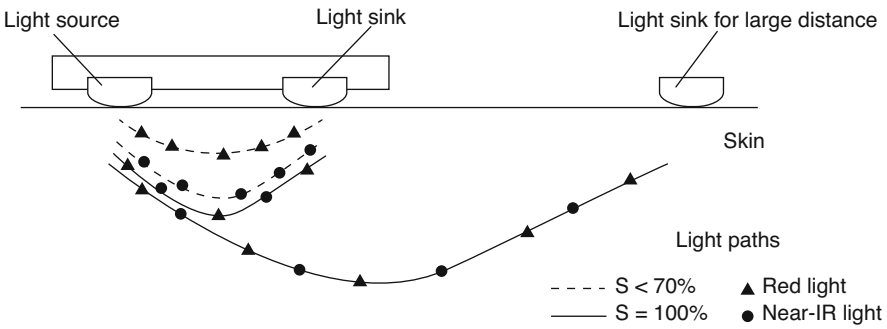

Fig. 12.41 Different arrangements of light source and sink for red and near-IR lights in reflection mode [35]

tissue, etc. The large volume of nonpulsatile arterial blood in the light path decreases the intensity of transmitted light. However, the transmitted light intensity passing through biological tissue experiences a relatively fast modulation from physiological point of view. The cardiac activity, respiratory activity, and blood oxygenation changes are basically responsible for the achievement of this fast modulation [35].

12.6.2 Sensing Aspects

The sensing aspects of the induced optic biomedical signal include transmitted light coupling with the light sink which is applied on the skin at a certain distance from the incident light source and its conversion into an electrical signal within light sink. In this way, the optic biomedical signals are registered with the help of transmitted incident light through tissues [35].

The fast fluctuations in local blood volume residing in the light propagation path modulate light absorption in tissue and slow fluctuations are present in the density of dominant chromophores in tissue. Due to this fact, there are three technologies which can mainly be used for the optic biomedical signals without considering the designed factor of optical sensors, namely, spectrometry, optical plethysmography, and optical oximetry [35].

In spectrometry, the light is absorbed by a chromophore in tissue which depends on the density of chromophore and the wavelength of applied light. Similarly, the light absorption spectrum gives a signature of the chromophore type as a function of wavelength. The amount of chromophore at the sensor is used for monitoring the local environment of the tissue [35].

The optical plethysmography detects the variations in the light absorption in tissue. The pulsating volume of arterial blood produces these variations in the illumination region due to transmitted light. The changing of optical path lengths

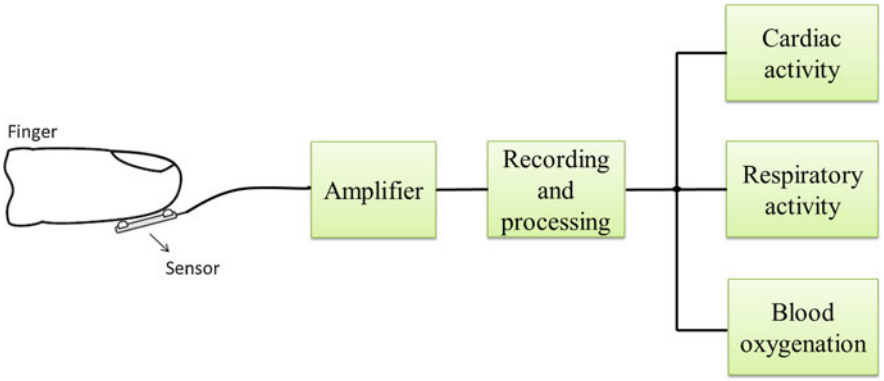

Fig. 12.42 Registration of optic biomedical signals from the finger in order to extract physiological parameters [35]

changes the total light absorption in the tissue. However, the total optical path length of the light beam is almost constant in tissue. The registered variations in the transmitted light intensity gives a signature of blood volume changes from the illumination region of transmitted light and these variations can be used for the monitoring of cardiac and respiratory activities [35].

The optical oximetry includes both existing technologies which are spectrometry and optical plethysmography for the assessment of blood oxygenation. In this technique, the level of the hemoglobin oxygen saturation in pulsatile arterial blood is calculated. The spectrometry technique in this method is used for evaluation of degree of hemoglobin oxygenation with the help of light absorption in the blood. On the other hand, the optical plethysmography is used for the separation of absorption by the pulsatile arterial blood from the nonpulsatile absorption with the help of the pulsatile nature of the transmitted light intensity. The registration of blood oxygenation during exploiting arterial pulsations is called pulse oximetry [35].

In spectrometry, the coefficient of absorption is the parameter of interest, whereas the path length is the parameter of interest for optical plethysmography [35].

The registration of optic biomedical signal for the extraction of physiological parameters, namely, cardiac activity, respiration activity, and blood oxygenation, is shown in Fig. 12.42. In Fig. 12.42, the optoplethysmogram signal is recorded from the finger in order to extract the physiological parameters. The amplifier is used to amplify the recorded signal, whereas the recording and processing block is used for the de-noising purpose. The recorded signal simultaneously offers the three different physiological parameters with multiparametric processing [35].

12.7 Analysis of Biomedical Signals

Biomedical signals are primarily used for the diagnosis and monitoring of specific pathological/physiological states. In some cases, the researchers have also used these signals for decoding and eventual modeling of specific biological systems. The recent advancement in technology allows the acquisition of multiple channels of biomedical signals. This process leads to additional signal processing challenges to identify meaningful interactions between these channels. The main aim of signal processing is generally noise removal, accurate signal modeling, extraction of components for analysis purpose, and feature extraction for deciding function or dysfunction of the heart and brain. The signal processing is used in biological applications due to several reasons. In most of the cases, the monitored biological signal contains an additive combination of signal and noise. The presence of noise can be due to instruments (sensors, amplifiers, filters, etc.) and electromagnetic interference (EMI). Therefore, the different conditions suggest different assumptions for noise characteristics, which will eventually lead to an appropriate choice of signal processing method [37].

12.7.1 Time-Domain Analysis

The time-domain analysis of biomedical signals is usually fast and easy to implement, because time-domain analysis does not need any transformation of biomedical signals. In time-domain analysis, several features based on different characteristics of signal are computed from biomedical signals. These time-domain features have been generally used in different areas of medical as well as engineering research. A major drawback of these features is due to the nonstationary nature of the biomedical signal, which changes the statistical properties over time. Therefore, the computed values of time-domain features may vary largely when the biomedical signal is recorded in interference and noisy environments. However, the time-domain features have been widely used for biomedical signal due to their lower computational complexity [38]. There are different time-domain characteristics which vary from one biomedical signal to the other.

In the time-domain analysis of EEG signals, the artifact which usually exceeded instantaneous amplitude as compared to normal instantaneous amplitude present in EEG signal is determined by amplitude thresholds. The muscle artifacts can be minimized with the use of slope or steepness threshold. The first-order derivative of EEG signal gives us the slope. In addition to first-order derivative, the second-order derivative is also used to measure the complexity present in EEG signal [30]. Apart from this measure, there are some other complexity measures such as fractal dimension and entropy which are also frequently used as features. The fractal dimension of the EEG signal decreases as the age increases in humans. Hence, it can be concluded with this fact that the fractal dimension is higher for a brain whose all

parts are active, but it is lower for an old brain whose parts are considerably less active. The same behavior is also recorded for the other complexity measures from EEG signals of older people as compared to younger people. This phenomenon is also true for a person suffering from diseases like epilepsy and Alzheimer's. The complexity measures decrease due to the presence of such kind of diseases. Moreover, the reduction of 30% fractal dimension is used as diagnosis criteria for epilepsy from EEG signals [30].

The most common feature in time-domain analysis of ECG signals is the duration of the heart cycle. The heart cycle duration is basically a time span from one R wave to the next occurring R wave. The other generally used features for ECG signal are the duration of QRS complex and the time interval between T and P waves. The QRS complex is determined by the characteristic shape and relative stable time constant in the pattern [30].

The time-domain analysis of EMG signals is possible with several features. The mean absolute value (MAV), root mean square (RMS), zero crossing, v order, log detector, waveform length (WL), Willison amplitude (WAMP), and slope sign change (SSC) are commonly used for the time-domain analysis of EMG signals. The MAV feature provides the information about energy and fatigue present in EMG signals. On the other hand, the RMS feature represents the non-fatigue as well as fatigue contraction. The frequency information present in EMG signals is provided by time-domain features such as zero crossing, WAMP, and SSC. The v- order and log detector features estimate the muscle contraction force and fatigue [39].

12.7.2 Frequency-Domain Analysis

The frequency-domain analysis of biomedical signals is possible with Fourier transform which converts the time-domain representation of a signal into frequency domain. The frequency-domain analysis is mainly used to characterize the frequency contents present in a signal. The major limitation of this technique is that the Fourier transform works only for stationary signals because the time information is lapsed in frequency-domain analysis.

In frequency-domain analysis of EEG signals, the main feature is the computation of power of the particular frequencies from the power spectra of the EEG signal. The spectral analysis of EEG signal will quickly identify any irregular pattern of higher harmonics in the frequency spectrum. The spectrum of EEG signal is generally analyzed only over a consecutive short-time segment. This short-time segment of EEG signal is known as "epoch." The length of epochs decides the frequency resolution of EEG signal in frequency spectrum. However, the selection of longer time segments will result in lower time resolution which is a trade-off between time and frequency resolution.

The frequency components of EEG signal such as alpha, beta, delta, and theta waves are very informative and it can be easily extracted from the power spectra

of the EEG signal. These frequency components are also used in the diagnostics of various diseases and disorders.

The analysis of EEG signals is also possible with frequency measure which is known as spectral edge frequency (SEF). This measure plays a significant role in the analysis of depth of anesthesia. It is found that a decrease in the value of SEF corresponds to a deeper level of anesthesia [30].

Similarly, median peak frequency (MPF) is another frequency measure in which frequency situated at 50% of the energy level is considered. The MPF gives the high-frequency contribution present in the frequency spectrum. This measure is also used in the analysis and classification of anesthesia depth [30].

In the frequency-domain analysis of ECG signal, the QRS complex is well localized in the high-frequency region. On the other hand, the low-frequency components are mainly due to P and T waves. The ST segment in the ECG signal mostly contains the low-frequency component. The frequency contents in a normal ECG signal and the deviating ECG signal have a significant difference because the normal heart rate is in the range of 60–100 beats per minute, whereas the fibrillation can exceed the range of 200 beats per minute. The depolarization and repolarization ramps in ECG signal are also changed under diseased conditions. This requires a much wider frequency bandwidth to identify different phenomena. The minor deviation of higher frequency in ECG signal creates a much larger number of harmonics which describe the frequency-domain features in the ECG signal. Therefore, a frequency span of 0–100 Hz usually represents normal ECG signal, whereas arrhythmias may require a high-frequency analysis up to 200 Hz. However, the high-frequency spectra will also be dominated by noise and it may not contribute any additional information [30].

A disease named as sinus tachycardia is also often detected in the frequency domain. A sinus tachycardia is detected when a sinus rhythm higher than 100 beats per minute appears. This similar condition may also occur during a physiological response to physical exercise or physical stress but it may lead to congestive heart failure in diseased cases. The case of sinus arrhythmia is also possible when the longest PP or RR intervals exceed the shortest interval by 0.16 s. This condition is frequent in teenage groups who have never suffered a heart disease [30].

The detection of fetal heart diseases using ECG signal during pregnancy is another area where the frequency-domain analysis plays a vital role. The ECG signals recorded from the leads placed on the abdomen of the mother are used to monitor the fetal heart diseases. The P and T waves obtained with the maternal ECG signal can easily be recognized in most cases. The maternal heart rate is usually lower than the fetal heart rate which is distinct from the mother's and the baby's ECG signals using filters designed in the frequency-domain.

The frequency-domain analysis of EMG signal leads to the fact that the frequency spectrum is mostly in the higher frequencies during fatigue, whereas the power spectrum is shifted toward lower frequencies after fatigue. This frequency shift indicates the muscle status such as rest and contraction states [30]. There are many features which are used for the frequency-domain analysis of EMG signals. The mean frequency (MF) measure is able to denote muscle fatigue during cyclic

dynamics. The median (MD) frequency measure is a universal index for muscle force and fatigue. The peak frequency (PF) feature is used for identifying fatigue state. The mean and total power features are also used for the identification of fatigue. The first, second, and third spectral moments are alternative statistical measures for fatigue identification. The frequency ratio is also used as a feature to distinguish between rest and contraction states of muscles [39].

12.7.3 Time-Frequency Domain-Based Analysis

The time-frequency domain analysis is widely used for the analysis of nonstationary signals because it provides time and frequency information together for a given signal. There are several time-frequency domain analysis methods such as short-time Fourier transform (STFT), wavelet transform (WT), and Wigner-Ville distribution (WVD) [40].

The time-frequency analysis is used for detecting spike-like epileptic patterns in EEG signals because these patterns appear for a short time period or random in most suspected epileptic EEG signals. Due to random occurrence of these patterns, the frequency-domain analysis does not provide exact time information for these patterns. The choice of epoch length is an important issue in time-frequency domain analysis of EEG signal. The epoch lengths of 1–2 s duration are usually recommended for time-frequency domain analysis of EEG signal. The epochs of this time duration may provide stability in data features [30].

The time-frequency analysis of ECG signal identifies the typical pattern or wave. The time-frequency analysis provides the separation of the mother's and baby's ECG signals. It should be noted that the waveform of the fetal ECG signal is analogous to adult ECG signal [30].

12.7.4 Other Methods

In real situations, most of the signals are nonlinear and nonstationary in nature. The analysis of such type of signals is a tedious task. The predefined basis function may fail to provide solutions. This problem can be overcome by an adaptive or signal-dependent basis which is used for the representation of nonlinear and nonstationary signals. A method named Hilbert-Huang transform (HHT) is an adaptive and empirical method. HHT consists of two parts for signal analysis. One of them is empirical mode decomposition (EMD) and the second one is Hilbert spectral analysis (HSA). This method provides good results for time-frequency-energy representations of many signals [41].

Another method for analysis of real signals is higher-order spectra (HOS). A real signal most specifically a non-Gaussian signal can be decomposed into higher-order spectral functions in which each higher-order spectral function may contain

different information about the signal [42]. These methods also provide significant contribution in biomedical signal analysis.

12.8 Modeling of Biomedical Signals

Biomedical signals can be modeled by mathematical functions. The procedure is started with finding a model which follows the laws of physics. The equations are solved for typical functions. The response of these equations is compared with developed physical model with the same typical functions. If these two responses are approximately equal, then we can use the developed model for analysis; otherwise, we have to improve our developed model [43].

12.8.1 Models for ECG Signal Representation

The ECG signals have pseudo-periodicity feature and features related to the constituent signals (P, QRS, and T). The modeling of ECG signals can be possible with parametric and nonparametric models. Most of them are parametric models such as impulse response of a pole-zero model and damped sinusoid model. The nonparametric models fail to exploit the nature of ECG signals. Hence, the parametric models overcome these problems.

The autoregressive (AR)/autoregressive moving-average (ARMA) model which is a parametric model is also used for the modeling of ECG signals. The amplitude-modulated (AM) sinusoidal signal model which is a special case of AR/ARMA model is also used due to its burst-like feature [44]. The model based on hidden Markov is also proposed to model every specific abnormal beat classification [45]. The dynamical model based on three coupled ordinary differential equations was used for generating synthetic ECG signals [46]. The Hilbert transform-based model is a recent approach for ECG signal modeling [47].

12.8.2 Models for EEG Signal Representation

The EEG signals have certain deviation or patterns as compared to the normal EEG signals during neurological disorders. These patterns occur for one or few seconds in the EEG signals. These patterns can be identified by modeling of EEG signals to detect various neurological diseases. The parametric modeling of EEG signal is the most common approach among them. The parametric model which is mostly used for EEG signal modeling is a rational transfer function with selected parameters. If the parameters lie in the denominator, then it is known as an all-pole or AR model, whereas if all the parameters lie in the numerator, then it is

known as all-zero or moving-average (MA) model. A model with parameters lie in the numerator and a denominator is known as pole-zero or ARMA model [48]. The parametric modeling of ictal EEG signal using Prony's method is also possible. This method is based on the assumption that the original signal is a sum of damped complex exponential sinusoids, and it has good frequency resolution compared to AR model. This method suggests that the modeling of ictal EEG signal is based on the poles of EEG signal [49]. A method based on second-order linear time-varying AR (TVAR) with appropriate chosen length obtained using FBSE is used for parametric modeling of EEG signal [17].

12.8.3 Models for EMG Signal Representation

The main purpose for modeling EMG signal is to understand electrophysiological information for the detection of neuromuscular disorders. The EMG signal modeling can also be possible by AR model [50]. A modified method autoregressive integrated moving-average (ARIMA) model has been also proposed for EMG signals in the literature [51].

12.8.4 Models of Other Biomedical Signals

The parametric modeling of PCG signals for the detection of murmurs is possible with AR modeling. This model used dominant poles for pattern classification and spectral tracking [52, 53].

The modeling of respiratory sound signals can be possible with mechanical as well as electrical models. In these models, the vocal and respiratory tract of humans can be represented by tubes and pipes and their electrical equivalent circuits [54].

12.9 Applications

The biomedical signals have also been used in certain areas of applications based on signal processing techniques such as detection of heart-related diseases, neurological disorders, neuromuscular diseases, postural stability analysis, and other related disease. The description of these applications is illustrated below.

12.9.1 Detection of Heart-Related Disorders

The heart-related signals are very useful to detect cardiovascular diseases. These detections are generally based on heart sounds and ECG signals. The detection of congestive heart failure (CHF) is carried out using eigenvalue decomposition from HRV signals extracted with ECG signals [55, 56]. The heart valve disorders can be classified with the method based on tunable-Q wavelet transform (TQWT) [57]. The diagnosis of arrhythmia using flexible analytic wavelet transform (FAWT) from ECG signals has significant importance [58]. The FAWT method is used for the detection of myocardial infarction (MI), which is a condition that indicates injury of the heart cell [59]. The automated detection system of CAD is developed with FAWT method using ECG signals [60]. In another work [61], the detection of CAD is also possible with HRV signals involving the FAWT. A method for diabetic patients using RR interval signals obtained from ECG signal is developed for screening [23].

12.9.2 Detection of Brain-Related Diseases

The brain-related diseases and disorders such as epilepsy, Alzheimer's, Parkinson's, and sleep disorder can be detected by EEG and MEG signals. The detection technique based on EMD method using EEG signals for epileptic seizure has been proposed [62]. The phase space representation of intrinsic mode functions has been also utilized to classify epileptic seizure EEG signals [63]. The second-order difference plot of intrinsic mode functions has been also used for epileptic seizure classification [64]. The entropy of intrinsic mode functions has been used for the automated detection of focal EEG signals [65]. The detection of ictal EEG signals using fractional linear prediction has been also proposed [66]. The sleep stages have been also classified using time-frequency image of EEG signals [67]. The iterative filtering method has been also used to develop an automated system for sleep stage classification [68].

12.9.3 Detection of Neuromuscular Diseases

The diagnosis of neuromuscular diseases has been also possible using computer-aided method. The technique based on wavelet neural network applied on EMG signals has been proposed for neuromuscular disorder detection [69]. A technique based on discrete wavelet transform for EMG signal classification with comparison of decision tree algorithms has been proposed [70]. The detection of muscle fatigue using EMG signals with time-frequency methods has been presented [71]. The fatigue during dynamic contractions of the muscle has been also detected using

EMG signals [72]. The automated classification of hand movements using TQWT-based filter bank with EMG signals has been also proposed [73].

12.9.4 Postural Stability Analysis

The postural control is very useful for everyday movement and the central nervous system provides sensory information for postural control. This system is used to maintain a proper postural balance. Any postural imbalance may lead to instability, falls, and injury. The center of pressure signals are commonly used to examine the postural control [74]. These signals can be analyzed with various signal processing methods. The method based on FBSE applied on the center of pressure signals has been used for postural stability analysis [74]. The method for assessment of standing postural stability in children has been also proposed [75]. The EMD method with second-order difference plots has been used for postural time-series analysis [76].

12.9.5 Other Related Applications

The knee joint pathological conditions change the vibroathrographic (VAG) signals. These VAG signals provide the abnormalities associated with knee joints**.** The automated screening of knee joints using double density dual-tree complex WT has been proposed [77]. The detection of direction of eyes movement has been possible using EOG signals [78]. This detection provides help to various disabled persons.

References

1. J. Enderle, J. Brozino, *Introduction to Biomedical Engineering* (Academic Press, Burlington, 2012)
2. O.G. Martinsen, S. Grimnes, *Bioimpedance and Bioelectricity Basics* (Academic Press, London, 2011)
3. R. Plonsey, R.C. Barr, *Bioelectricity: a Quantitative Approach* (Springer Science & Business Media, New York, 2007)
4. A. Winter, *Biomechanics and Motor Control of Human Movement* (Wiley, Hoboken, 2009)
5. G.S. Firestein, R. Budd, S.E. Gabriel, I.B. McInnes, J.R. O'Dell, *Kelley's Textbook of Rheumatology E-Book* (Elsevier Health Sciences, London, 2012)
6. A.P. Turner, J.C. Pickup, Diabetes mellitus: biosensors for research and management. Biosensors **1**(1), 85–115 (1985)
7. L.J. Blum, P.R. Coulet, *Biosensor Principles and Applications* (M. Dekker, New York, 1991)
8. T. Vo-Dinh, B. Cullum, Biosensors and biochips: advances in biological and medical diagnostics. Fresenius J. Anal. Chem. **366**(6–7), 540–551 (2000)
9. J.-Y. Yoon, *Introduction to Biosensors: from Electric Circuits to Immunosensors* (Springer, Cham, 2016)

10. A.V. Oppenheim, A.S. Willsky, S.H. Nawab, *Signals and Systems*, 2nd edn. (Prentice Hall, Upper Saddle River, 1997)
11. S. Mukhopadhyay. NPTEL (2016). [Online]. http://textofvideo.nptel.ac.in/108105088/lec7.pdf
12. S.R. Devasahayam, *Signals and Systems in Biomedical Engineering* (Springer US, Boston, 2000)
13. J. Schroeder, Signal processing via Fourier-Bessel series expansion. Digit. Signal Process. **3**(2), 112 (1993)
14. S. Gupta, K.H. Krishna, R.B. Pachori, M. Tanveer, Fourier-Bessel series expansion based technique for automated classification of focal and non-focal EEG signals, in *International Joint Conference on Neural Networks (IJCNN)*, 2018, pp. 1–6
15. A.S. Hood, R.B. Pachori, V.K. Reddy, P. Sircar, Parametric representation of speech employing multi-component AFM signal model. Int. J. Speech Technol. **18**(3), 287–303 (2015)
16. R.B. Pachori, Discrimination between ictal and seizure-free EEG signals using empirical mode decomposition. Res. Lett. Signal Process. **14**, 2008 (2008)
17. R.B. Pachori, P. Sircar, EEG signal analysis using FB expansion and second-order linear TVAR process. Signal Process. **88**(2), 415–420 (2008)
18. R.B. Pachori, P. Sircar, A new technique to reduce cross terms in the Wigner distribution. Digit. Signal Process. **17**(2), 466–474 (2007)
19. R.B. Pachori, P. Sircar, Analysis of multicomponent AM-FM signals using FB-DESA method. Digit. Signal Process. **20**(1), 42–62 (2010)
20. R.B. Pachori, P. Avinash, K. Shashank, R. Sharma, U.R. Acharya, Application of empirical mode decomposition for analysis of normal and diabetic RR-interval signals. Expert Syst. Appl. **42**(9), 4567–4581 (2015)
21. S. Sood, M. Kumar, R.B. Pachori, U.R. Acharya, Application of empirical mode decomposition–based features for analysis of normal and CAD heart rate signals. J. Mech. Med. Biol. **16**(1), 1640002 (2016)
22. P. Jain, R.B. Pachori, Time-order representation based method for epoch detection from speech signals. J. Intell. Syst. **21**(1), 79–95 (2012)
23. R.B. Pachori, M. Kumar, P. Avinash, K. Shashank, U.R. Acharya, An improved online paradigm for screening of diabetic patients using RR-interval signals. J. Mech. Med. Biol. **16**(1), 1640003 (2016)
24. R.B. Pachori, P. Sircar, *Non-stationary Signal Analysis: Methods Based on Fourier-Bessel Representation* (LAP LAMBERT Academic Publishing, Germany, 2010)
25. A. Bhattacharyya, L. Singh, R.B. Pachori, Fourier–Bessel series expansion based empirical wavelet transform for analysis of non-stationary signals. Digit. Signal Process. **78**, 185–196 (2018)
26. R.G. Andrzejak et al., Indications of nonlinear deterministic and finite-dimensional structures in time series of brain electrical activity: Dependence on recording region and brain state. Phys. Rev. E 64 **6**, 061907 (2001)
27. M.V. Gils, Lecture 01: Introduction and recapitulation of essential techniques (2015). [Online]. https://mycourses.aalto.fi/course/view.php?id=9367&lang=fi
28. B. Mulgrew, P. Grant, J. Thompson, *Digital Signal Processing: Concepts and Applications* (Macmillan Education London, 1999)
29. V. Singh, K. Veer, R. Sharma, S. Kumar, Comparative study of FIR and IIR filters for the removal of 50 Hz noise from EEG signal. Int. J. Biomed. Eng. Technol. **22**(3), 250–257 (2016)
30. K. Najarian, R. Splinter, *Biomedical Signal and Image Processing* (CRC Press, Boca Raton, 2005)
31. A.L. Goldberger et al., PhysioBank, PhysioToolkit, and PhysioNet: components of a new research resource for complex physiologic signals. Circulation **101**(23), e215–e220 (2000)
32. M. Tangermann et al., Review of the BCI competition IV. Front. Neurosci. **6**, 55 (2012)
33. R.M. Rangayyan, *Biomedical Signal Analysis*, vol 33 (Wiley, Hoboken, 2015)
34. E. Kaniusas, *Biomedical Signals and Sensors I* (Springer, Berlin, Heidelberg, 2012)
35. E. Kaniusas, *Biomedical Signals and Sensors II* (Springer, Berlin, Heidelberg, 2015)

36. G. Keiser, *Biophotonics – Concepts to Applications* (Springer Singapore, Singapore, 2016)
37. M. Kutz, *Standard Handbook of Biomedical Engineering and Design* (McGraw-Hill, New York, 2003)
38. A. Phinyomark, P. Phukpattaranont, C. Limsakul, Feature reduction and selection for EMG signal classification. Expert Syst. Appl. **39**(8), 7420–7431 (2012)
39. T.N.S. Tengku Zawawi et al., A review of electromyography signal analysis techniques for musculoskeletal disorders. Indones. J. Electr. Eng. Comput. Sci. **11**(3), 1136 (2018)
40. B. Boashash, *Time-Frequency Signal Analysis and Processing: a Comprehensive Reference* (Academic Press, Amsterdam, 2015)
41. N.E. Huang, *Hilbert-Huang Transform and Its Applications*, vol 16 (World Scientific, Hackensack, 2014)
42. C.L. Nikias, J.M. Mendel, Signal processing with higher-order spectra. IEEE Signal Process. Mag. **10**(3), 10–37 (1993)
43. C.L. Phillips, J.M. Parr, E.A. Riskin, *Signals, Systems, and Transforms* (Prentice Hall, Upper Saddle River, 1995)
44. S. Mukhopadhyay, P. Sircar, Parametric modelling of ECG signal. Med. Biol. Eng. Comput. **34**(2), 171–174 (1996)
45. R.V. Andreao, B. Dorizzi, J. Boudy, ECG signal analysis through hidden Markov models. IEEE Trans. Biomed. Eng. **53**(8), 1541–1549 (2006)
46. P.E. McSharry, G.D. Clifford, L. Tarassenko, L.A. Smith, A dynamical model for generating synthetic electrocardiogram signals. IEEE Trans. Biomed. Eng. **50**(3), 289–294 (2003)
47. J.-C. Nunes, A. Nait-Ali, Hilbert transform-based ECG modeling. Biomed. Eng. **39**(3), 133–137 (2005)
48. J. Pardey, S. Roberts, L. Tarassenko, A review of parametric modelling techniques for EEG analysis. Med. Eng. Phys. **18**(1), 2–11 (1996)
49. O.A. Elsayed, A. Eldeib, F. Elhefnawi, Parametric modeling of ICTAL epilepsy EEG signal using Prony method. Int. J. Comput. Sci. Softw. Eng. (IJCSSE) **3**(1), 86–89 (2014)
50. D. Graupe, K.H. Kohn, A. Kralj, S. Basseas, Patient controlled electrical stimulation via EMG signature discrimination for providing certain paraplegics with primitive walking functions. J. Biomed. Eng. **5**(3), 220–226 (1983)
51. M.H. Sherif, R.J. Gregor, J. Lyman, Effects of load on myoelectric signals: the ARIMA representation. IEEE Trans. Biomed. Eng. **5**, 411–416 (1981)
52. A. Iwata, N. Suzumura, K. Ikegaya, Pattern classification of the phonocardiogram using linear prediction analysis. Med. Biol. Eng. Comput. **15**(4), 407–412 (1977)
53. A. Iwata, N. Ishii, N. Suzumura, K. Ikegaya, Algorithm for detecting the first and the second heart sounds by spectral tracking. Med. Biol. Eng. Comput. **18**(1), 19–26 (1980)
54. Z. Moussavi, Fundamentals of respiratory sounds and analysis. Synth. Lect. Biomed. Eng. **1**(1), 1–68 (2006)
55. R.R. Sharma, A. Kumar, R.B. Pachori, U.R. Acharya, Accurate automated detection of congestive heart failure using eigenvalue decomposition based features extracted from HRV signals. Biocybern. Biomed. Eng. **39**, 312 (2019)
56. M. Kumar, R.B. Pachori, U.R. Acharya, Use of accumulated entropies for automated detection of congestive heart failure in flexible analytic wavelet transform framework based on short-term HRV signals. Entropy **19**(3), 92 (2017)
57. S. Patidar, R.B. Pachori, Classification of heart disorders based on tunable-Q wavelet transform of cardiac sound signals, in *Chaos Modeling and Control Systems Design*, (Springer, Cham, 2015), pp. 239–264
58. M. Kumar, R.B. Pachori, U.R. Acharya, Automated diagnosis of atrial fibrillation ECG signals using entropy features extracted from flexible analytic wavelet transform. Biocybern. Biomed. Eng. **38**(3), 564–573 (2018)
59. M. Kumar, R.B. Pachori, U.R. Acharya, Automated diagnosis of myocardial infarction ECG signals using sample entropy in flexible analytic wavelet transform framework. Entropy **19**(9), 488 (2017)

60. M. Kumar, R.B. Pachori, U.R. Acharya, Characterization of coronary artery disease using flexible analytic wavelet transform applied on ECG signals. Biomed. Signal Process. Control **31**, 301–308 (2017)
61. M. Kumar, R.B. Pachori, U.R. Acharya, An efficient automated technique for CAD diagnosis using flexible analytic wavelet transform and entropy features extracted from HRV signals. Expert Syst. Appl. **63**, 165–172 (2016)
62. V. Bajaj, R.B. Pachori, Classification of seizure and nonseizure EEG signals using empirical mode decomposition. IEEE Trans. Inf. Technol. Biomed. **16**(6), 1135–1142 (2012)
63. R. Sharma, R.B. Pachori, Classification of epileptic seizures in EEG signals based on phase space representation of intrinsic mode functions. Expert Syst. Appl. **42**(3), 1106–1117 (2015)
64. R.B. Pachori, S. Patidar, Epileptic seizure classification in EEG signals using second-order difference plot of intrinsic mode functions. Comput. Methods Prog. Biomed. **113**(2), 494–502 (2014)
65. R. Sharma, R.B. Pachori, U.R. Acharya, Application of entropy measures on intrinsic mode functions for the automated identification of focal electroencephalogram signals. Entropy **17**(2), 669–691 (2015)
66. V. Joshi, R.B. Pachori, A. Vijesh, Classification of ictal and seizure-free EEG signals using fractional linear prediction. Biomed. Signal Process. Control **9**, 1–5 (2014)
67. V. Bajaj, R.B. Pachori, Automatic classification of sleep stages based on the time-frequency image of EEG signals. Comput. Methods Prog. Biomed. **112**(3), 320–328 (2013)
68. R. Sharma, R.B. Pachori, A. Upadhyay, Automatic sleep stages classification based on iterative filtering of electroencephalogram signals. Neural Comput. & Applic. **28**(10), 2959–2978 (2017)
69. A. Subasi, M. Yilmaz, H.R. Ozcalik, Classification of EMG signals using wavelet neural network. J. Neurosci. Methods **156**(1–2), 360–367 (2006)
70. E. Gokgoz, A. Subasi, Comparison of decision tree algorithms for EMG signal classification using DWT. Biomed. Signal Process. Control **18**, 138–144 (2015)
71. A. Subasi, M.K. Kiymik, Muscle fatigue detection in EMG using time–frequency methods, ICA and neural networks. J. Med. Syst. **34**(4), 777–785 (2010)
72. M. Gonzalez-Izal et al., EMG spectral indices and muscle power fatigue during dynamic contractions. J. Electromyogr. Kinesiol. **20**(2), 233–240 (2010)
73. A. Nishad, A. Upadhyay, R.B. Pachori, U.R. Acharya, Automated classification of hand movements using tunable-Q wavelet transform based filter-bank with surface electromyogram signals. Futur. Gener. Comput. Syst. **93**, 96–110 (2019)
74. R.B. Pachori, D. Hewson, Assessment of the effects of sensory perturbations using Fourier–Bessel expansion method for postural stability analysis. J. Intell. Syst. **20**(2), 167–186 (2011)
75. G.F. Harris, S.A. Riedel, D. Matesi, P. Smith, Standing postural stability assessment and signal stationarity in children with cerebral palsy. IEEE Trans. Rehabil. Eng. **1**(1), 35–42 (1993)
76. R.B. Pachori, D. Hewson, H. Snoussi, J. Duchêne, Postural time-series analysis using empirical mode decomposition and second-order difference plots, in *International Conference on Acoustics, Speech and Signal Processing (ICASSP 2009)*, 2009, pp. 537–540
77. M. Sharma, P. Sharma, R.B. Pachori, V.M. Gadre, Double density dual-tree complex wavelet transform-based features for automated screening of knee-joint vibroarthrographic signals, in *Machine Intelligence and Signal Analysis*, (Springer, Singapore, 2009), pp. 279–290
78. M. Merino, O. Rivera, I. Gómez, A. Molina, E. Dorronzoro, A method of EOG signal processing to detect the direction of eye movements, in *First International Conference on Sensor Device Technologies and Applications (SENSORDEVICES)*, 2010, pp. 100–105